

1 **Controls on dissolved organic matter (DOM)**
2 **degradation in a headwater stream: the influence of**
3 **photochemical and hydrological conditions in**
4 **determining light-limitation or substrate-limitation of**
5 **photo-degradation**

6
7 **R. M. Cory,¹ K.H. Harrold,¹ B. T. Neilson², G.W. Kling³**

8 [1] {University of Michigan, Earth & Environmental Science, Ann Arbor, Michigan}

9 [2] {Utah State University, Civil and Environmental Engineering, Utah Water Research
10 Laboratory, Logan, Utah}

11 [3] {University of Michigan, Department of Ecology & Evolutionary Biology, Ann Arbor,
12 Michigan}

13 Correspondence to: R. M. Cory (rmcory@umich.edu)

14
15 **Abstract**

16 We investigated how absorption of sunlight by chromophoric dissolved organic matter (CDOM)
17 controls the degradation and export of DOM from Innavaik Creek, a beaded stream in the
18 Alaskan Arctic. We measured concentrations of dissolved organic carbon (DOC), as well as
19 concentrations and characteristics of CDOM and fluorescent dissolved organic matter (FDOM),
20 during ice-free periods of 2011-2012 in the pools of Innavaik Creek and in soil waters draining
21 to the creek. Spatial and temporal patterns in CDOM and FDOM in Innavaik Creek were
22 analyzed in conjunction with measures of DOM degradation by sunlight and bacteria and
23 assessments of hydrologic residence times and in-situ UV exposure. CDOM was the dominant
24 light attenuating constituent in the UV and visible portion of the solar spectrum, with high
25 attenuation coefficients ranging from $86 \pm 12 \text{ m}^{-1}$ at 305 nm to $3 \pm 1 \text{ m}^{-1}$ in the
26 photosynthetically active region (PAR). High rates of light absorption and thus light attenuation
27 by CDOM contributed to thermal stratification in the majority of pools in Innavaik Creek under

1 low-flow conditions. In turn, thermal stratification increased the residence time of water and
2 DOM, and resulted in a separation of water masses distinguished by contrasting UV exposure
3 (i.e., UV attenuation by CDOM with depth resulted in bottom waters receiving less UV than
4 surface waters). When the pools in Innavait Creek were stratified, DOM in the pool bottom
5 water closely resembled soil water DOM in character, while the concentration and character of
6 DOM in surface water was reproduced by experimental photo-degradation of bottom water.
7 These results, in combination with water column rates of DOM degradation by sunlight and
8 bacteria, suggest that photo-degradation is the dominant process controlling DOM fate and
9 export in Innavait Creek. A conceptual model is presented showing how CDOM amount and
10 lability interact with incident UV light and water residence time to determine whether photo-
11 degradation is “light-limited” or “substrate-limited”. We suggest that degradation of DOM in
12 CDOM-rich streams or ponds similar to Innavait is typically light-limited under most flow
13 conditions. Thus, export of DOM from this stream will be less under conditions that increase the
14 light available for DOM photo-degradation (i.e., low flows, sunny days).

15 **1 Introduction**

16 The decomposition of dissolved organic matter (DOM) to CO₂ and its subsequent
17 transport to and release from surface waters is an important process in the carbon cycling of
18 inland waters (e.g., Cole et al., 1994, 2007; Kling et al., 1991). This decomposition has been
19 mainly attributed to bacterial respiration in the water column and sediments (e.g., Battin et al.,
20 2009; Cole et al., 2007; Wetzel, 2001). Exposure to ultraviolet (UV) light is also a key control
21 on the photochemical conversion of DOM to CO₂ in surface waters (e.g., Cory et al., 2007;
22 Moran et al., 2000; Vähätalo and Wetzel, 2008), and coupled photochemical and microbial
23 processing can enhance DOM degradation beyond the effect of bacteria or light alone (Cory et
24 al., 2013; Judd et al., 2007; Tranvik and Bertilsson, 2001).

25 Recent work demonstrated that in shallow arctic lakes and streams the photo-degradation
26 of DOM can greatly exceed bacterial respiration, accounting for up to 94% of the total DOM
27 processed in the water column (Cory et al., 2014). The water column rate of DOM photo-
28 degradation to CO₂ (photo-mineralization) or to partially degraded DOM (e.g., photo-stimulated
29 bacterial respiration; Cory et al., 2013) depends on (1) the amount of UV radiation from sunlight
30 reaching the water surface, (2) the absorption of UV light by chromophoric DOM (CDOM), and

1 (3) the apparent quantum yield, a term quantifying the lability of DOM as moles of product
2 formed per moles of photons absorbed by DOM. Water column rates of DOM photo-
3 degradation increase linearly with increasing UV light reaching the water surface, or with
4 increasing photo-lability of DOM. However, the rate of DOM photo-degradation in the water
5 column depends non-linearly on CDOM concentrations and depth due to attenuation of light
6 mainly by CDOM with depth in the water column (Hu et al., 2002; Miller, 1998).

7 As CDOM concentrations increase, the depth of UV light penetration decreases to
8 shallower depths, but the average rate of light absorption by CDOM increases in the water
9 column (Hu et al., 2002). Thus, while the depth of UV light penetration is low, on the order of
10 10 to 100 cm in the streams and small ponds in the Arctic characterized by high concentrations
11 of CDOM (Cory et al., 2007, 2014; Gareis et al., 2010; Prairie et al., 2009; Watanabe et al.,
12 2011), the rate of light absorption by CDOM may be high. If the light absorption rate is high
13 enough, photo-degradation rates of DOM reach an asymptote such that increasing CDOM has no
14 effect on photo-degradation integrated through the water column (Hu et al., 2002). At this point,
15 where photo-degradation is insensitive to changing CDOM concentrations, the system is ‘light
16 limited’ – in a light-limited system, as the amount of incident UV light increases so does the rate
17 of photo-degradation. In contrast, in very clear waters light attenuation by CDOM is low and
18 rates of DOM photo-degradation are limited by insufficient CDOM to absorb the available light
19 – in these ‘substrate-limited’ systems, increasing the incident UV light has no effect but higher
20 CDOM concentrations increase rates of photo-degradation. Thus, depending on the incident
21 light available, the CDOM concentrations, and the depth of the water column, the rates of DOM
22 degradation in surface waters may be either light-limited, substrate-limited, or co-limited by light
23 and substrate. To our knowledge, the range of conditions and the interactions of controls on
24 photo-degradation across the continuum of light- versus substrate-limitation have not been
25 described or characterized.

26 At the scale of a stream reach, lake, or catchment, DOM degradation is related to both
27 photochemical processing and the influence of hydrology on light exposure. Water residence
28 times in a stream or river are generally a function of watershed and channel characteristics, but
29 may also be influenced by surface and subsurface transient storage (e.g., (Chapra and Runkel,
30 1999; Neilson et al., 2010; Zarnetske et al., 2011) and thermal stratification that can isolate water
31 masses (e.g., Merck and Neilson, 2012). While the influence of these factors on biogeochemical

1 processes and solute concentrations has been studied (e.g., Boano and Harvey, 2014; Miller et
2 al., 2009), the relative importance of CDOM concentration and lability, UV exposure, and water
3 residence times on the degradation of DOM is unknown for stream or lake ecosystems.

4 Running waters, and especially lower-order streams, may be expected to have relatively
5 low DOM degradation in the water column due to their high flow rates and short water residence
6 times. Although small streams are often shallow and if unshaded by riparian vegetation may
7 have light penetration to the bottom, the water residence time in any given reach is short and
8 therefore there is little time for substantial photo-degradation of DOM. However, in areas of low
9 relief, the headwater streams have longer residence times and greater light exposure through a
10 shallow water column. In the Arctic, residence times within low gradient, first-order beaded
11 streams are controlled by thermal stratification of the beads (pools) (Merck et al. 2012, Merck
12 and Neilson 2012). Strong thermal stratification (up to 10 °C temperature difference within 0.5
13 m depth) observed in Imnavait Creek on the North Slope of Alaska was attributed to a
14 combination of high concentrations of CDOM, low wind stress at the stream surface, underlying
15 frozen soils, and low in-stream discharge (Merck et al. 2012). Because sunlight is rapidly
16 attenuated in high-CDOM waters, warming by solar radiation is restricted to surface layers and
17 can cause strong thermal stratification and density gradients (Fee et al., 1996; Houser, 2006;
18 Kling, 1988). Merck et al. (2012) found that this stratification isolated the pool surface water
19 from the bottom water and increased the water residence times in a reach from minutes under
20 mixed conditions to hours or weeks when the pools were stratified. At the same time, there were
21 distinct gradients in the concentrations of chromophoric and fluorescent fractions of dissolved
22 organic matter (CDOM and FDOM, respectively) between pool surface and bottom waters
23 (Merck et al. 2012). The authors suggested that these gradients in CDOM and FDOM were due
24 to photo-degradation of DOM in the surface waters, and that stratification regulated the residence
25 times of water and DOM and thus controlled the extent of DOM degradation in this stream.

26 To quantify the role of photo-degradation in producing observed DOM gradients in
27 stratified stream pools, and to generally determine the influence of in-stream stratification, water
28 residence times, and UV exposure on DOM degradation, we measured the lability and rates of
29 DOM degradation by sunlight and bacteria along with changes in CDOM and FDOM within the
30 pools of Imnavait Creek in two summers with differing discharge and stratification patterns. We
31 demonstrate that photo-degradation is the dominant process altering DOM chemistry and

1 producing CO₂ in the water column of this headwater stream under all conditions, and we show
2 how rates of photo-degradation are governed by the amount and lability of DOM (CDOM), light
3 attenuation, patterns of stratification, and residence time. We suggest that in relatively shallow,
4 high CDOM headwater streams, DOM photo-degradation is limited by available light instead of
5 by available substrate (DOM) under a wide range of hydrological conditions.

6 **2 Methods**

7 **2.1 Site description**

8 Imnavait Creek is a headwater, beaded stream located on the North Slope of Alaska in a
9 glacial valley formed during the Sagavanirktok glaciation in the Kuparuk River basin (68.616
10 °N, 149.318 °W; (Detterman et al., 1958; Hamilton, 1986). The creek primarily lies in the
11 organic soil layer and only occasionally cuts through to the mineral soil (McNamara et al., 1998).
12 The connected pools, or beads, were formed by the erosion and melting of large ice deposits that
13 had underlain the creek (McNamara et al., 1998; Walker et al., 1989) .

14 Previous studies of Imnavait Creek found that spring snowmelt accounts for 23 to 75 % of
15 the watershed's annual water flux(Kane et al., 2004; McNamara et al., 2008) compared to 6 to 9
16 % produced by the largest, single summer storm events (McNamara et al., 2008). Subsurface
17 water paths are limited to the thawed active layer as the region is underlain with up to several
18 hundred meters of permafrost, which effectively separates the active layer from any deep ground
19 water (Osterkamp and Payne, 1981). Typical seasonally-thawed active layer depths at Imnavait
20 ranged from 25 to 40 cm, occasionally extending to 100 cm (Hinzman et al., 1991). Water
21 inputs from the riparian zone occur through both surface and diffuse subsurface flow(Kane et al.,
22 2000). In addition to surface chutes that connect the stream pools, water travels between pools
23 through the riparian zone with both subsurface flow through the active layer and surface flow
24 during significant precipitation events (Merck and Neilson, 2012).

25 We studied a ~120 m reach of the creek consisting of a series of seven pools connected by
26 short chutes (Fig. 1). Pools were named starting with pool 1 and proceeding downstream
27 sequentially to pool 7. Across these 7 pools, surface areas ranged from 2 to 129 m², volumes
28 ranged from 0.2 to 102 m³, and pool depths were between ~0.21 – 2 m. Along the reach of
29 creek studied, we collected soil water from a water track that drains from the adjacent eastern
30 hillslope into the pools. Seventeen sites were sampled along the water track from the hill top to

1 the valley bottom along the water track with distances between sites ranging from 30 to 190 m.
2 Soil water was also collected from an array of 55 sites within a 150 m by 90 m grid in a riparian
3 zone on the eastern hillslope adjacent to the study pools in Innavait Creek (Fig. 1).

4 **2.2 Water sample collection**

5 Water samples were collected from the surface and bottom of the seven pools monthly
6 from 23 June through 4 August 2011, and weekly from 27 June through 18 August 2012. Pool
7 water was collected from the surface and bottom of each pool through MasterFlex[®] tubing (Cole-
8 Parmer, Vernon Hills, IL) using a peristaltic pump (GeoPump Inc., Medina, NY). Soil water
9 was collected from the 17 sites in the water track flowing into the pools (Fig. 1), once in June
10 and twice each in July and August in both 2011 and 2012, and from the riparian zone adjacent to
11 the study pools monthly from June through August 2011. From the water track or riparian area,
12 soil water was withdrawn using stainless-steel soil needles inserted into the soil, through
13 MasterFlex[®] tubing, into plastic syringes. Temperature, conductivity, and pH were measured
14 from pool and soil water at the time of collection using WTW meters (models 3210; Xylem,
15 White Plains, NY). All pool and soil water samples were filtered in the field into high-density
16 polyethylene bottles and kept cool and dark until analysis. Aliquots for analysis of DOM
17 quantity and quality were filtered through pre-combusted Whatman GF/F glass fiber filters
18 (Whatman, Clifton, NJ).

19 ***Sunlight attenuation***

20 Light attenuation with depth was measured in pools 1, 2, 3, and 6 on 27 June 2011 and in
21 pools 1, 2, 3, 6 and 7 on 23 June 2012 using a compact optical profiling system for UV light in
22 natural waters (UV C-OPS; Biospherical Instruments Inc., San Diego, CA) as previously
23 described (Cory et al., 2013, 2014). The C-OPS measured downwelling cosine-corrected
24 irradiance at 7 wavebands (305, 313, 320, 340, 380, 395, and 412 nm) and photosynthetically
25 active radiation (PAR, 400-700 nm). Attenuation coefficients ($K_{d,\lambda}$) were calculated from the
26 downwelling irradiance (E_λ) as a function of depth (z) at each waveband:

$$27 \quad E_{\lambda,z} = E_{\lambda,0} e^{-K_{d,\lambda} z} \quad (1)$$

1 From multiple casts in each pool ($n = 2$ to 5), the coefficient of variation of $K_{d,\lambda}$ ranged from 1 to
2 3 % in the UV and 9 % for PAR. Means \pm standard error (SE) of K_d are reported.

3 **2.3 In-situ monitoring**

4 Temperature sensor arrays (HOBO[®] Water Temp Pro v2; Onset Computer Corporation,
5 Inc., Bourne, MA) were deployed vertically in each pool ($n = 1$ to 5 per pool in 2011 and $n=3-25$
6 per pool in 2012) from late-June through mid-August, measuring at 5 minute intervals. The
7 probes were wrapped with aluminum foil to prevent radiation-caused heating (Neilson et al.,
8 2010) and placed starting 5 to 15 cm from the bottom of the pool and then at intervals ranging
9 from 5 to 50 cm. Additional monitoring of pool 2 was conducted for one week in July 2011 and
10 for most of July and part of August in 2012 where two sondes were deployed near the surface
11 and bottom of the pool with oxygen, pH, specific conductance, and temperature probes (YSI
12 6920 V2 sonde with ROX[™] optical dissolved oxygen, 6561 pH, 6560 conductivity, and 6560
13 temperature sensors; YSI Inc., Yellow Springs, OH) measuring at 15 minute intervals. Finally,
14 discharge data were collected at a weir further downstream to compare and contrast the flow
15 variability between summer 2011 and 2012 (Kane and Hinzman, 2011; Kane, 2015).

16 **2.4 Meteorological measurements**

17 Air temperature 1 m above the ground and precipitation were measured hourly at a
18 meteorological station on the west-facing ridge of the Innavait Creek basin approximately 1 km
19 upstream of the study site using a temperature probe (model HMP45C; Campbell[®] Scientific,
20 Logan, UT) and tipping bucket rain gauge, respectively (Kane and Hinzman, 2011). Global
21 solar, UVA and UVB radiation were each measured at five minute intervals at Toolik Field
22 Station (TFS, 11 km West of Innavait at 68.616 °N, 149.318 °W) with pyranometers from Kipp
23 & Zonen (CMP-6) and Yankee Environmental System, Inc. (UVB-1 and UVA-1), respectively.
24 The global solar pyranometer measured a spectral range of 310 to 2800 nm, while UVB and
25 UVA pyranometers measured 280-320 nm and 320-400 nm, respectively. Photosynthetically
26 active radiation (PAR; 400-700 nm) was measured hourly using a quantum sensor by Li-Cor (LI-
27 190S) at the same location.

1 2.5 DOM quantity and quality

2 Samples for dissolved organic carbon (DOC) concentration were acidified with trace-metal
3 grade hydrochloric acid to approximately pH 3 after filtration through Whatman GF/F filters and
4 stored in the dark at 4 °C until analysis using a high-temperature platinum-catalyzed combustion
5 followed by infrared detection of CO₂ (Shimadzu TOC-V; Shimadzu, Columbia, MD).

6 The chromophoric and fluorescent fractions of DOM (CDOM and FDOM, respectively)
7 were analyzed within hours to at most several days of collection. Samples were stored in the
8 dark at 4 °C until warmed to room temperature (20 to 25 °C) just prior to analysis. UV-Vis
9 absorbance spectra of CDOM were collected using 1-cm path length quartz cuvettes with a
10 spectrophotometer (USB 2000+UV-VIS; Ocean Optics, Inc., Dunedin, FL or Aqualog; Horiba
11 Scientific). Sample absorption was measured against laboratory-grade deionized (DI) water
12 blanks (Barnstead E-Pure and B-Pure; Barnstead Thermolyne, Dubuque, IA). The spectral slope
13 ratio (S_R) was calculated from the absorbance spectrum of each sample as the ratio of the slope
14 from 275 to 295 nm to the slope from 350 to 400 nm (Helms et al., 2008). CDOM absorption
15 coefficients ($a_{CDOM,\lambda}$) were calculated as follows:

$$16 \quad a_{CDOM,\lambda} = \frac{A_\lambda}{l} 2.303 \quad (2)$$

17 where A is the absorbance reading at wavelength λ and l is the pathlength in meters.
18 $SUVA_{254}$ was calculated as absorbance at 254 nm divided by the cuvette pathlength (m) and then
19 divided by the DOC concentration (mg C L^{-1} ; Weishaar et al., 2003).

20 Excitation-emission matrices (EEMs) were measured on all water samples with a
21 Fluoromax-4 fluorometer or an Aqualog (Horiba Scientific, Edison, NJ) following previously
22 described procedures (Cory et al., 2010). An aliquot of sample was placed in the 1-cm quartz
23 cuvette for each EEM and diluted with DI if necessary to bring $A_{254} < 0.6$. EEMs were corrected
24 for inner-filter effects and for instrument-specific excitation and emission corrections in Matlab
25 (version 7.7) following Cory et al. (Cory et al., 2010). The fluorescence index (McKnight et al.,
26 2001) was calculated from each corrected EEM as the ratio of emission intensity at 470 nm over
27 the emission intensity at 520 nm at an excitation wavelength of 370 nm (Cory et al., 2010).
28 Emission intensity at FDOM peaks A, C, and T was evaluated at excitation/emission pairs
29 250/450, 350/450, 275/340 (nm/nm), respectively, in Raman Units (RU; Stedmon et al., 2003).

1 2.6 DOM degradation

2 Water collected from Innavait Creek in amber HDPE bottles in the field was used for
3 photochemical and bacterial degradation experiments, as described in Cory et al. (2014).
4 Briefly, dark bacterial respiration was measured from whole water samples incubated for five to
5 seven days in the dark at 6-7 °C alongside killed controls (1% HgCl₂) in air-tight, pre-combusted
6 12-mL borosilicate exetainer vials (Labco, Inc). For DOM photo-degradation, GF/F filtered
7 water was placed in air-tight, pre-combusted 12-mL borosilicate exetainer vials and exposed to
8 natural sunlight at Toolik Field Station for ~12 hours alongside foil-wrapped dark controls at
9 temperatures ranging from 10-16 °C. Bacterial re-growth experiments for photo-stimulated
10 bacterial respiration were conducted as described in Cory et al. (2013, 2014). There were four
11 independent replicates from each water sample for every analysis type and treatment. Membrane
12 inlet mass spectrometry (MIMS) was used to measure bacterial or photochemical oxygen
13 consumption relative to killed or dark controls, respectively. Bacterial or photochemical
14 production of CO₂ during complete oxidation (mineralization) of DOM was quantified as
15 production of dissolved inorganic carbon (DIC) relative to killed or dark controls, respectively,
16 using a DIC analyzer (model AS-C3, Apollo SciTech, Inc.). After exposure to sunlight or
17 bacteria, subsamples were analyzed for CDOM and FDOM as described above. Changes in
18 DOM quality are reported as mean ± standard error (SE) of the four replications of each
19 treatment.

20 We used previously reported lability and rates of DOM degradation by bacteria and
21 sunlight in Innavait Creek, measured from experiments described above, during our study
22 periods in 2011 and 2012 to determine the sensitivity of DOM degradation in Innavait Creek to
23 photochemical and hydrological factors. The conversion of experimental measures of DOM
24 degradation to water column rates of degradation is described for Innavait Creek and other
25 waters in the Arctic in Cory et al. (2013, 2014). In the current study, we quantified how rates of
26 DOM photo-degradation in the water column varied with available light, CDOM concentrations,
27 and lability of DOM measured in Innavait Creek during the 2011-2012 summer seasons.

28 The integrated, water-column rate of DOM photo-degradation is:

29
$$Photo - degradation (mol C m^{-2} d^{-1}) = \int_{\lambda_{min}}^{\lambda_{max}} \phi_{\lambda} Q_{dso,\lambda} (1 - e^{-K_{d\lambda}z}) \frac{a_{CDOM\lambda}}{a_{tot\lambda}} d\lambda \quad (3),$$

1 where λ_{\min} and λ_{\max} are the minimum and maximum wavelengths of light contributing to the
2 photo-degradation of DOC (280 and 700 nm, respectively). Φ_{λ} is the apparent quantum yield
3 spectrum for photo-degradation of DOM (mol product mol⁻¹ photons absorbed nm⁻¹; a measure
4 of DOM lability to photo-degradation which decreases exponentially with increasing
5 wavelength). We used previously reported spectra of DOM lability (Φ_{λ}) in Innavait Creek for
6 photo-mineralization DOC to CO₂ and photo-stimulated bacterial respiration (Cory et al. 2014).
7 $Q_{dso,\lambda}$ is the spectrum of the UV from sunlight that reaches the water surface (accounting for
8 reflection; Cory et al. 2014). $Q_{dso,\lambda}$ varies by location (latitude/longitude), time of day, date, and
9 sunny vs. cloudy sky conditions, as described in Cory et al. 2014. $K_{d,\lambda}$ is the attenuation
10 coefficient with depth (Eqn. 1). $a_{CDOM,\lambda}$ is the concentration of CDOM measured as described
11 above (Eqn. 2). $a_{CDOM,\lambda}/a_{tot,\lambda}$ is the spectrum of the ratio of absorption by CDOM to the total
12 absorption (where $a_{tot,\lambda}$ is the total absorption in the water column due to CDOM, particles, and
13 water). The ratio of $a_{CDOM,\lambda}/a_{tot,\lambda}$ was assumed to be 1 at all wavelengths (i.e., CDOM was the
14 main UV-absorbing constituent in Innavait Creek; Cory et al. 2014).

15 From Eqn. 3, it follows that as DOM lability to photo-degradation (Φ_{λ}) or incoming UV
16 light ($Q_{dso,\lambda}$) increase, the depth-integrated or areal water-column rate of DOM photo-
17 degradation increases. In addition, photo-degradation of DOM throughout the water column
18 increases with increasing $K_{d,\lambda}$ up to a point where at high $K_{d,\lambda}$ the relationship is asymptotic (Fig.
19 S1). This is because while increasing CDOM provides more DOM to absorb light and photo-
20 degrade, the absorption of UV light by CDOM also controls light attenuation (i.e., $a_{CDOM,\lambda} \approx K_{d,\lambda}$
21 ; presented in the *Results* section below). Thus as light attenuation ($K_{d,\lambda}$) increases, at some
22 point light becomes limiting and adding more CDOM (increasing K_d) results in no change in the
23 integrated water column rate of photo-degradation (Fig. S1). In this study, we used the range of
24 terms in Eqn. 3 observed in Innavait Creek (Fig. S2) to develop a conceptual model of controls
25 on DOM photo-degradation in this and similar systems. For example, we used the range of
26 $Q_{dso,\lambda}$ spectra for Innavait Creek representing the average, minimum and maximum UV light
27 reaching the surface of Innavait Creek over the course of the day during the study period, as
28 well as the average, minimum and maximum of $a_{CDOM,\lambda}$ observed in Innavait Creek.

29 **3 Results**

1 **3.1 Meteorological Conditions**

2 There was no difference in mean air temperatures between the mid-June through mid-
3 August study periods in 2011 vs. 2012 at Imnavait Creek. However, June-August was generally
4 sunnier and drier in 2011 compared to 2012 (Table 1). The total global solar radiation (310-2800
5 nm) and total UV and visible photon flux (280-700 nm) were 17 % and 24 % higher,
6 respectively, in 2011 compared to 2012 (Table 1, Fig. S3). Precipitation was three times greater
7 during the summer 2012 compared with 2011, and the lower precipitation in 2011 resulted in
8 significantly lower volume of water passing the weir in 2011 versus 2012 (Table 1, Fig. S1).

9 **3.2 Pool stratification and separation of water masses**

10 Light attenuation coefficients ($K_{d,\lambda}$) in Imnavait Creek decreased exponentially with
11 increasing wavelength from $88 \pm 12 \text{ m}^{-1}$ at 305 nm to $17 \pm 3 \text{ m}^{-1}$ at 412 nm to $3 \pm 1 \text{ m}^{-1}$ in the
12 photosynthetically active region (PAR). In most pools, there was no significant difference
13 between in-situ $K_{d,\lambda}$ values and CDOM absorption coefficients ($a_{\text{CDOM},\lambda}$) collected from filtered
14 water from the same pool at the time $K_{d,\lambda}$ was measured (as shown for 320 nm and 412 nm in
15 Fig. 2). These results demonstrate that in most pools CDOM was the dominant light absorbing
16 constituent in the water column (Fig. 2), consistent with low particulate matter concentrations in
17 this stream and previous work showing that CDOM dominates UV light absorption in these
18 streams (Cory et al. 2014). However, in two pools sampled in June 2011, the in-situ $K_{d,\lambda}$ values
19 at 320 nm were significantly higher than the corresponding CDOM absorption coefficients
20 measured from filtered water (Fig. 2). This was likely due to the inherent challenges deploying
21 an instrument to quantify $K_{d,\lambda}$ in the UVB range in high CDOM waters where 99 % of light at
22 320 nm is attenuated by ~ 8 cm (based on the mean $K_{d,\lambda}$ or CDOM coefficients in Fig. 2).

23 Five of the seven pools (2, 3, 5, 6, 7) were repeatedly thermally stratified with a nearly 10
24 °C temperature difference between top and bottom waters during sunny and dry (low-flow)
25 conditions in Imnavait Creek (Figs. 3 and 4). In contrast, pools 1 and 4 did not exhibit
26 stratification in 2011 or 2012. During the sunnier and drier summer of 2011, pools 2, 3, 5, 6, 7
27 were stratified on 43 to 46 out of 50 days measured (Fig. 3), while during the wetter summer of
28 2012, these pools stratified only 11 out of 49 days measured (Fig. 4). Within each summer, the
29 roles of solar radiation and precipitation were evident in the frequency and extent of stratification
30 in each pool. For example, pools 2, 3, 5, 6, and 7 showed the greatest extent of thermal

1 stratification once the discharge from snowmelt had receded, coinciding with the period when
2 solar irradiance was highest (e.g., late June in 2011 and 2012; Figs. 3, 4). In addition, during
3 both summers a portion of each stratified pool mixed nightly due to surface heat loss, followed
4 by re-stratification with increasing solar irradiance during the day (Merck and Neilson, 2012).
5 Following substantial precipitation events, stream flow increased and caused stratified pools to
6 mix completely within hours of precipitation, as demonstrated for example after a rain even on
7 17 July 2011 (Fig. 3). After mixing, pools stratified again within four to five days (Fig. 3).

8 Under stratified conditions, water and DOM in the pools experienced contrasting UV
9 exposure. For example, Pool 3 had a depth of 1.4 m from the water surface to the sediment, and
10 on average the depth of the surface mixing layer was 50 cm (ranging from 20 – 50 cm below the
11 water surface; Fig. 3). It follows that DOM below 50 cm was in the “bottom water”, defined as
12 water trapped below the diel mixing depth during stratified conditions. The depth of UVB and
13 UVA light penetration was always less than 50 cm in Innavait Creek. For example, using the
14 mean CDOM absorption coefficients at 320 nm and 412 nm (Fig. 2), 99 % of all incoming UVB
15 and UVA light was absorbed within 8 ± 1 cm and 35 ± 3 cm, respectively (average \pm SE;
16 maximum depth of UVA penetration observed was 45 cm based on attenuation coefficients at
17 412 nm in Fig. 2). Therefore, DOM in the surface of the pools experienced UV light exposure
18 each day while DOM trapped in pool bottom waters was protected from UV light during
19 stratified conditions.

20 **3.3 Stream and soil water chemistry**

21 Both the pool water and the soil water draining into Innavait Creek had low pH, low
22 conductivity, and high concentrations of DOC, CDOM, and FDOM (Table 2). The pH ranged
23 from 5.2 ± 0.1 to 5.7 ± 0.1 and the conductivity ranged from 25 ± 10 to 12 ± 2 $\mu\text{S cm}^{-1}$ in soil
24 and pool water, respectively. DOC concentrations ranged from 1412 ± 78 and 785 ± 13 $\mu\text{M C}$ in
25 pool and soil water, respectively, during summer of 2012 (Table 2). CDOM and FDOM proxies
26 for the chemical composition of soil and pool water DOM were consistent with a terrestrial
27 source of DOM, i.e., high molecular weight, aromatic compounds derived from degradation of
28 plant and soil organic matter. For example, in the soil waters draining to Innavait Creek, the
29 spectral S_R , a proxy for average molecular weight of DOM (Helms et al. 2008) was 0.75 ± 0.08 ,
30 and the specific UV absorbance at 254 nm ($SUVA_{254}$), strongly correlated with aromatic C

1 content, was $4.4 \pm 0.1 \text{ L mg C}^{-1} \text{ m}^{-1}$. The fluorescence index, a proxy for DOM source and
2 aromatic C content, was 1.59 ± 0.07 . Although there were some significant differences in mean
3 values between soil and pool water DOC, CDOM and FDOM (discussed below), similar ranges
4 of DOC, CDOM and FDOM were observed for the pool bottom waters in Innavait Creek and
5 for the soil water draining into the pool bottoms (Table 2).

6 There were no significant differences in average pH, conductivity, DOC, CDOM, or
7 FDOM concentrations in the soil waters between 2011 and 2012 (Table 2). There was no
8 difference in average optical character of soil water DOM between summers except for
9 SUVA_{254} , which was significantly lower in the soil waters in 2012 compared to 2011 (Table 2).
10 In contrast, there were significant differences in DOM quality between 2011 and 2012 when
11 comparing pool bottom or surface water across years (Table 2), likely due to differences in the
12 extent of stratification between years.

13 When the pools in Innavait Creek were stratified, there were significant differences in
14 water chemistry between pool surface and bottom water. In-situ data collected under stratified
15 conditions in Pool 2 from 8 - 15 July 2011 showed significantly higher dissolved oxygen in the
16 surface compared to the bottom pool water (Fig. 3). Discrete water samples collected when
17 pools were stratified in 2011 and 2012 showed significantly higher concentrations of DOC,
18 CDOM, and FDOM in bottom waters compared to surface waters (as shown in Fig. 5 for pools
19 sampled on 14 July 2011). The surface waters of most pools sampled under stratified conditions
20 had different DOM quality compared to bottom waters, as indicated by significantly lower
21 SUVA_{254} , higher S_R , and lower FI (Table 3; Fig. 5). When the stream pools stratified, DOM in
22 pool bottom water was not significantly different than soil water for most CDOM and FDOM
23 measures or DOM quantity and quality (Table 3). In contrast, when the pools were mixed, there
24 were no significant differences in DOC, CDOM, and FDOM between pool surface and bottom
25 waters (e.g., as shown in Fig. 5 for pools sampled on 21 July 2012).

26 **3.4 Photochemical degradation of DOM**

27 Previous work showed that photo-mineralization of DOM to CO_2 accounted for the
28 majority of DOM degradation in Innavait Creek ($24.69 \pm 18.28 \text{ mmol C m}^{-2} \text{ d}^{-1}$, mean \pm SE;
29 Cory et al. 2014). Here we show that in addition to mineralization of DOM, exposure of
30 Innavait Creek DOM to ~12 hours of sunlight altered the chemical quality of the remaining

1 DOM, likely due to preferential mineralization of the aromatic fraction (Cory et al., 2007;
2 Stubbins et al., 2010) and to partial photo-oxidation of the DOM (Cory et al., 2013, 2014).
3 These photochemical alterations of DOM resulted in a significant loss of CDOM and FDOM at
4 each wavelength compared to dark controls (12.1 ± 1.4 % to 27.2 ± 2.1 % less CDOM or FDOM
5 compared to the dark control depending on CDOM wavelength or FDOM peak, Table 4).
6 Because there was greater loss of CDOM at long wavelengths compared to shorter wavelengths,
7 photo-degradation significantly increased the S_R by 15.8 ± 1.3 % and decreased the FI by $-11.7 \pm$
8 0.8 % on average. There was an increase in peak T intensity by 4.1 ± 1.5 % for photo-exposed
9 DOM compared to dark controls (Table 4).

10 Photo-degradation of DOM enhanced the respiration of bacteria fed the photo-exposed
11 DOM (compared to DOM kept in the dark); the water column rate of photo-stimulated bacterial
12 respiration was 3.04 ± 1.31 mmol C m⁻² d⁻¹ (Cory et al. 2014). Relative to the initial photo-
13 exposed DOM, bacterial incubation generally increased CDOM and FDOM (from 3 ± 1 to 15 ± 1
14 %, Table 4). The exception was that following bacterial degradation of the photo-exposed
15 DOM, there was a 12 ± 1 % loss of peak T fluorescence (Table 4). Coupled photo and bacterial
16 degradation increased the fluorescence index by 5 ± 1 % (Table 4).

17 **3.5 Bacterial degradation of DOM**

18 The average areal rate of dark bacterial respiration of DOM integrated over the mean
19 depth (0.5 m) in Innavait Creek was 2.35 ± 0.34 mmol O₂ m⁻² d⁻¹. Bacterial degradation
20 resulted in significant loss of CDOM and FDOM compared to the killed control over the six day
21 incubation period at 6 - 7 °C (-2.9 ± 1.6 % to -7.6 ± 2.4 %, Table 4). There was no detectable
22 change in the S_R or the FI after dark bacterial degradation of DOM compared to the killed
23 control (Table 4).

24 **4 Discussion**

25 **4.1 Stratification in beaded streams**

26 Stratification is likely widespread during the summer in beaded pools and small ponds
27 across the Arctic. Stratification in tundra ponds is well documented (Boano and Harvey, 2014;
28 Hobbie, 1980), as are the factors conducive to stratification including high light attenuation by
29 CDOM (Cory et al., 2007, 2014; Gareis et al., 2010; Watanabe et al., 2011), adequate solar

1 radiation, and in streams low wind stress at the surface and low enough discharge coupled with
2 permafrost below the stream (Merck and Neilson, 2012; Merck et al., 2012; this study). For
3 example, nearly one third of both lower-order streams and coastal plain lakes sampled in the
4 Alaskan Arctic had average CDOM absorption coefficients at 305 nm greater than or equal to the
5 absorption coefficients observed in the surface of Innavait Creek (Cory et al., 2014), consistent
6 with high CDOM absorption coefficients reported in streams and small ponds and lakes across
7 the Arctic (Gareis et al., 2010; Watanabe et al., 2011). While fewer studies have reported in-situ
8 $K_{d,\lambda}$ values compared to reports of CDOM absorption coefficients in arctic freshwaters, strong
9 agreement between $K_{d,\lambda}$ and $a_{\text{CDOM},\lambda}$ in this and other studies (Fig. 2; Cory et al., 2014; Gareis et
10 al., 2010; MORRIS et al., 1995) demonstrate that CDOM was the main UV and visible (PAR)
11 light absorbing constituent in surface waters across the Arctic. Because UV and PAR account
12 for approximately 51 % of the energy within the shortwave radiation portion of the spectrum
13 (300 - 2500 nm), absorption of sunlight by CDOM contributes to the frequency and extent of
14 stratification by restricting warming to the surface layers (Caplanne and Laurion, 2008; Merck
15 and Neilson, 2012).

16 Given that there was no significant difference in the average CDOM absorption
17 coefficients in pool surface waters between 2011 and 2012 (Table 3), or between pool bottom
18 water temperatures or in wind stress (Table 1), differences in the extent and frequency of
19 stratification in the pools between years were most likely due to differences in discharge (Table
20 1; Fig. S1). Low in-stream discharges common in 2011 were due to significantly less
21 precipitation than in 2012. Low discharge led to low turbulence, allowing for more common
22 thermal stratification in the pools throughout a large fraction of the open water season (Table 1,
23 Fig. 3). The higher flows during summer 2012 resulted in approximately five-fold greater stream
24 volume compared to 2011, which increased the turbulence that induced frequent mixing
25 throughout the water column in the pools (Table 1; Fig. 4).

26 **4.2 DOM composition and photo-degradation**

27 There are three lines of evidence in support of photo-degradation as the main control on
28 the observed differences in DOM quantity and composition between pool surface and bottom
29 waters in Innavait Creek under stratified conditions: (1) water column rates of photo-
30 mineralization of DOM and photo-stimulated bacteria respiration each exceeded dark bacterial

1 respiration (Cory et al. 2014; Table 4), (2) experimental photo-degradation of Imnavait DOM
2 closely reproduced the depth differences in DOM concentration and composition (Table 4), and
3 (3) depth differences in DOM concentration and composition were consistent with effects of
4 sunlight on DOM observed in other studies.

5 The mean water column rate of photo-mineralization of DOM to CO₂ was about ten times
6 faster than photo-stimulated bacterial respiration or dark bacterial respiration in Imnavait Creek
7 (Cory et al. 2014, Table 4). Thus, although 99 % of all UVB and UVA light causing photo-
8 mineralization of DOM was attenuated within 8 to 35 cm below the pool surface, respectively
9 (Fig. 2), thereby confining photo-degradation of DOM to the top ~ 35 cm of the pool, photo-
10 mineralization in this surface layer was fast enough to exceed rates of bacterial respiration
11 occurring throughout the UV-exposed and UV-protected portions of the water column (Table 4).

12 The second line of evidence in support of photo-degradation as the dominant process
13 creating differences in DOM character between surface and bottom waters was that photo-
14 degradation experiments reproduced the magnitude and direction of depth differences in DOC,
15 CDOM, and FDOM observed under stratified conditions (Tables 2 and 4, Fig. 5). Compared to
16 pool bottom waters, surface waters had significantly lower CDOM and FDOM concentrations,
17 higher S_R, and lower FI, by 9 to 55 % (Tables 2 and 4, Fig. 5). Exposure of bottom water to ~12
18 hours of natural sunlight resulted in a comparable loss of CDOM and FDOM, and similarly
19 higher S_R, and lower FI (11 to 27 % loss or change in CDOM or FDOM compared to dark
20 controls; Table 4). Thus, DOM in pool surface waters and in photo-exposed bottom waters had
21 lower concentrations of aromatic DOM (i.e., CDOM and FDOM) with lower average molecular
22 weight compared to DOM protected from UV in the bottom waters. Many studies have
23 demonstrated that photo-degradation of DOM results in a loss of CDOM and FDOM Granéli et
24 al., 1996), a decrease in aromaticity (Brooks et al., 2007; Stubbins et al., 2010), and a decrease in
25 average molecular weight (e.g., S_R, Cory et al., 2007; Helms et al., 2008; Spencer et al., 2010),
26 just as we observed.

27 It is unlikely that bacterial processing of DOM could produce similar changes to those
28 observed between surface and bottom waters or to the results of photo-degradation experiments.
29 Bacteria degrade stream DOM and decrease CDOM and FDOM (Cory and Kaplan, 2012), but, at
30 the same time some bacterial processes can regenerate CDOM and FDOM (e.g., Amado et al.,

1 2006; Moran et al., 2000), leading to a net balance between degradation and regeneration. In our
2 experiments the dark bacterial degradation of DOM resulted in a net loss of CDOM and FDOM,
3 but the loss was much lower compared to photo-degradation (e.g., ~ 2 to 8 % decrease over six
4 days, Table 4). Furthermore, bacterial degradation had no detectable effect on the S_R or FI, and
5 thus cannot explain the significant differences in S_R and FI between surface and bottom waters
6 in Innavait Creek (Tables 2, 3 and 4, Fig. 5).

7 In an earlier study of Innavait Creek, Merck et al. (2012) found that soil water FDOM
8 was chemically similar to pool bottom water FDOM. Cold soil water from subsurface lateral
9 flows plunged into the pool bottom during stratified conditions, bringing in FDOM that remained
10 relatively unchanged in composition from the FDOM in soil waters. In our study we show that,
11 similarly, FDOM but also pH, conductivity, DOC, and CDOM are comparable in quantity or
12 quality between soil waters and pool bottom waters (Tables 2 and 3). These results suggest that
13 either DOM in soil waters draining into isolated pool bottoms experiences little degradation in
14 the pool, as would be expected based on relatively slow rates of bacterial respiration in cold,
15 acidic, low nutrient, and often anoxic water (Table 4, Fig. 3-4), or that the pathways, rates, and
16 fate of DOM degradation in both soils and bottom waters are similar.

17 **4.3 Synthesis of factors controlling DOM degradation**

18 Given that photochemical processes dominate the degradation and alteration of DOM in
19 Innavait Creek, estimates of DOM degradation or export at a stream reach or whole catchment
20 scale must be based on an integration of the photochemical and hydrological controls on DOM
21 degradation. These controls include (1) the amount of surface UV available to be absorbed by
22 CDOM ($Q_{dso,\lambda}$, Eqn. 3), (2) the amount of CDOM to absorb and attenuate UV light in the water
23 column ($a_{CDOM,\lambda}$ and K_d ; Eqn. 3), (3) the lability of DOM to photo-degradation, quantified as
24 apparent quantum yields (Φ_λ ; Eqn. 3), and (4) the residence time of DOM in the water column or
25 in a stream reach as affected by flow rates and stratification that in turn control the total UV light
26 exposure and amount of DOM photo-degradation. These main controls and their feedbacks are
27 summarized in Fig. 6, which shows that as light exposure increases, DOM photo-degradation
28 increases. Similarly, there are different pathways through which increased CDOM can affect
29 light exposure. First, higher CDOM increases light attenuation and thus helps facilitate thermal
30 stratification. Stratification in turn results in increased water residence times that can increase

1 the opportunity for light exposure and photo-degradation. For example, in pool surface waters
2 where light exposure is greatest, during the day under low-flow conditions nearly the entire
3 upper layer is stratified (Fig. 3), which increases residence time and light exposure (right side of
4 Fig. 6). Second, although increasing CDOM increases light attenuation, the effect on light
5 exposure can vary (left side of Fig. 6). In general, if K_d is relatively low and light penetrates to
6 the bottom of the water column, increasing CDOM will result in greater total light exposure of
7 DOM in the system, and thus greater total light absorption by CDOM to drive photochemical
8 reactions. However, if K_d is relatively high and light is extinguished well before it reaches the
9 bottom of the water column, the system is light-limited and adding more CDOM will not
10 increase the overall light exposure of DOM (or light absorption by CDOM). The relative
11 importance of these scenarios can be estimated by first examining the sensitivity of various
12 components in the photo-degradation model (Eqn. 3).

13 To investigate the sensitivity of DOM photo-degradation to the amount of surface UV,
14 CDOM, or Φ_λ , we varied each term independently in the equation for the water column rate of
15 DOM photo-mineralization (Eqn. 3), using the average, minimum, and maximum values
16 observed in Imnavait Creek (Fig. S2). Holding surface UV and Φ_λ constant (using the average
17 observed values) and varying CDOM across the range observed in the pool surface waters of
18 Imnavait Creek (39 to 63 m^{-1} at 305 nm, mean of 53 ± 2 ; Table 2), there was little variation in
19 water column rates of photo-mineralization (Fig. 7). This result indicates that photo-degradation
20 of DOM in Imnavait Creek is represented by higher K_d and falls in the asymptotic range shown
21 in Fig. S1, meaning it is limited by insufficient UV light. It follows that increasing UV light
22 (while holding CDOM and Φ_λ constant), should significantly increase the rate of DOM photo-
23 mineralization, as shown in Fig. 7. That is, the daily total surface UV light varied by nearly 10-
24 fold over the course of the summer season due to differences in solar zenith angle or cloud cover
25 (as shown for 2012 in Fig. S3), and thus there was a nearly 10-fold higher rate of photo-
26 mineralization when using the maximum vs. minimum surface UV light available in Eqn. 3 (Fig.
27 7). The greatest effect on the rate of photo-degradation occurred when holding the UV light and
28 CDOM to their average values, and varying the lability of DOM to photo-mineralization (i.e.,
29 varying Φ_λ). In this case, with a 6 to 20-fold range in Φ_λ (depending on wavelength; Fig. S2),
30 DOM was converted to CO_2 by sunlight ~ 13-fold faster using the maximum vs. the minimum
31 observed Φ_λ (Fig. 7).

1 The second step in understanding photo-degradation for any system is to consider the
2 integrated effects of light attenuation with flow rates, stratification, and anticipated residence
3 time distributions. Integrating the photochemical and hydrological factors produces a continuum
4 of conditions that can represent or classify any particular system (Fig. 8a,b). For example, as
5 light exposure and residence times increase, the amount of DOM lost through photo-
6 mineralization increases (Fig. 8a). However, the quantity and photo-lability (*quality*, Φ_λ) of
7 CDOM both determine the rates and the total amount of DOM photo-degradation. In systems
8 with high CDOM concentrations or low light exposure, photochemical processes can be light
9 limited rather than substrate (CDOM) limited. In such systems waters are rarely photo-bleached
10 clear before inputs from soil waters or sediments replenish the CDOM lost to photo-degradation.
11 This is the situation in Imnavait Creek (e.g., Table 3; Fig. 8a, left side;), which applies to most
12 arctic headwater catchments or any system that receives high inputs of organic matter (Koehler
13 et al., 2014). Similarly, if the photo-lability (and thus the Φ_λ) of the DOM is low (the lower,
14 dashed line on Fig. 8a), then more UV is required for photo-degradation, and the system would
15 be again considered light-limited. This is likely the case in the lower-CDOM Kuparuk River
16 (spectral characteristics described in Cory et al. 2014), a fourth-order stream where it is joined by
17 Imnavait Creek, although under some situations this river may be co-limited by light and
18 substrate. Most of the waters in the Alaskan Arctic would fall in between these examples on this
19 conceptual diagram, based on CDOM concentrations and Φ_λ values (Cory et al. 2014). In these
20 cases where DOM photo-degradation is light-limited, the amount of time the DOM is exposed to
21 UV becomes more important than the mass of DOM exposed. On the other hand, if photo-
22 lability is very high and CDOM concentrations are very low, then the system is substrate-limited
23 and the total mass of DOM exposed is more important than the amount of time the DOM spends
24 exposed to UV (Fig. 8a, right side). This is because when the system is substrate limited, even a
25 short exposure to UV will result in rapid and substantial photo-degradation, and exposing greater
26 amounts of DOM even over short residence times will increase the overall photochemical
27 processing in the system. Similarly, as one moves further right on Fig. 8a, the DOM loss as a
28 percentage of initial amount declines once the system has switched from light- to substrate-
29 limitation.

30 Finally, the nature and controls on DOM photo-degradation of a river reach (or whole
31 system) can be expressed as a function of light attenuation and residence times (Fig. 8b). When

1 water is flowing quickly through a stream the residence times are very short and the water
2 column is well mixed, DOM spends less time exposed to UV light, and even at medium to low
3 values of CDOM and K_d the system is light-limited (Fig. 8a,b left) and DOM loss to photo-
4 mineralization is low (Fig. 8a left). At the other extreme, low flow conditions create long
5 residence times, and even at medium values of CDOM the system is substrate-limited (Fig. 8b,
6 right) and again DOM photo-mineralization may become low (Fig. 8a, right).

7 The relationship between residence time and DOM photo-degradation in Imnavait Creek
8 was explored by multiplying *Eqn. 3* (representing the water column rate of DOM
9 photodegradation as the product of UV light, CDOM, and Φ_λ) by residence time to generate the
10 results in Fig. 9. Combinations of minimum and maximum values of incident UV light, CDOM,
11 and Φ_λ were used to create a ‘lowest case’ and ‘highest case’ scenario of photo-degradation over
12 a range of residence time from hours to 20 days. Thus, Fig. 9 shows cumulative DOM loss as a
13 function of residence for a range of conditions (i.e., UV light availability, CDOM, and Φ_λ)
14 generated using a ‘lowest case’ and ‘highest case’ scenario of photo-degradation. Because it was
15 shown in Fig. 7 (left set of bars) that the natural variability in CDOM concentrations has no
16 effect on water column rates of photo-degradation, the scenarios were created by varying
17 incoming UV light and DOM quality (Φ_λ). For example, the minimum UV light and minimum
18 Φ_λ values observed resulted in low rates of photo-mineralization; over a 20 day residence time
19 less than 5% of the DOM in surface waters could be converted to CO₂ by photo-mineralization.
20 Conversely, combining the maximum UV light and maximum Φ_λ values shows that 100% of the
21 DOM could be converted to CO₂ by photo-mineralization at the end of about one week (Fig. 9).
22 However, a precise estimate of residence time is difficult to achieve in practice given that there
23 are inputs of water and “fresh” (labile) CDOM as a parcel of water moves downstream;
24 accounting for these inputs is needed to quantify the total, integrated amount of DOM broken
25 down by light as a function of residence time in a stream.

26 In all surface waters there is a variety of combinations of photochemical and hydrological
27 controls that vary in space and time, and that define the “range” of DOM photo-degradation
28 rates. For example, in Imnavait Creek longer residence times occur during times of low flow and
29 stratification, and this stratification serves to protect DOM from UV light by isolating water
30 masses in pool bottoms (e.g., Table 3, Fig. 5). The volume of water sequestered in the pool
31 bottoms (below the mixing depth) under stratified conditions was on average about 70% of the

1 total pool volume (Figs. 3, 4; Merck et al. 2012). Thus, under stratified conditions, the majority
2 of the pool volume was sequestered in the bottom, below the depth of UV light penetration (8 –
3 45 cm see results section 3.2). However, the depth of light penetration into the ponds does not
4 differ between stratified (low flow) or mixed (high flow) conditions as shown by the limited
5 differences in $a_{\text{CDOM}\lambda}$ values at 305 nm between these conditions in Innavait Creek (comparing
6 pool surface $a_{\text{CDOM}\lambda}$ values in 2011 vs. 2012, Table 3). Thus, the amount of CDOM exposed to
7 light, or the rate of light absorption, does not differ between stratified vs. mixed conditions (for a
8 given amount of sunlight under given sky conditions). The only difference is the amount of time
9 for the photo-degradation to occur (greater photo-degradation under longer residence times
10 associated with low-flow, stratified conditions; Fig. 9). Therefore, although most water was
11 sequestered in the pool bottoms under stratified conditions, more DOM is lost due to photo-
12 degradation under these conditions. This is because there is enough light-absorbing DOM that is
13 labile to photo-degradation even in the pool surface waters under all conditions that DOM photo-
14 degradation is not limited by substrate (DOM supply). The amount of water and DOM
15 sequestered in the bottom waters does not influence the amount of DOM that can be degraded by
16 light in this system.

17 Rates of photo-mineralization varied little over the narrow range of CDOM observed in
18 the surface waters of Innavait Creek (Fig. 7, left), and because CDOM was very high
19 photochemical reactions were light-limited (Fig. 8b). In addition, the consistently high CDOM
20 concentrations observed across space (pool to pool) and averaged over time (2011 to 2012) in
21 Innavait Creek (Tables 2 and 3, Fig. 5) suggests that CDOM lost to photo-mineralization under
22 any photochemical or hydrological conditions is rapidly replenished from riparian soil waters
23 over relatively short time periods (see also Merck et al. 2012). It is likely that stream reaches
24 with high CDOM concentrations (substrate rich) and residence times in the range observed in
25 Innavait Creek are similarly always light-limited (Fig. 8). Increased residence times, or lower
26 CDOM concentrations such as those observed in the Kuparuk River, will move a system from
27 light-limitation toward co-limitation by light and substrate (Fig. 8), again depending on the
28 combination of photochemical and hydrological properties and their variability in space and
29 time.

30 **5 Conclusions**

1 Results from this study demonstrate that in Innavait Creek photo-degradation dominates
2 over bacterial degradation of DOM, and photo-degradation can create substantial differences in
3 DOM chemistry between water masses isolated during stratification. The amount and lability of
4 CDOM and the light attenuation by CDOM form a critical control point in DOM degradation –
5 higher CDOM attenuates light faster with depth but results in no change or an increase in the
6 overall rate of light absorption in the water column. With increasing CDOM and thus increasing
7 rates of light-absorption, photo-degradation rates in the water column are more likely to be light-
8 limited and rates will increase with incident UV light or residence time. Given that higher light
9 attenuation by CDOM traps heat in surface waters and creates stratification, which lengthens
10 residence times and thus the time-integrated light exposure of DOM, low-flow conditions in
11 Innavait Creek likely maximize the conditions for photo-degradation of DOM.

12 On the other hand, if CDOM concentrations are very low, then the system is substrate-
13 limited and the total mass of DOM exposed is more important than the amount of time the DOM
14 spends exposed to UV (Fig. 8a, right side). This is because when the system is substrate limited,
15 even a short exposure to UV will result in rapid and substantial photo-degradation, and exposing
16 greater amounts of DOM even over short residence times will increase the overall photochemical
17 processing in the system. In addition, in our conceptual model the lability of DOM to photo-
18 degradation acts as a control on processing rates independent of whether a system is light- or
19 substrate limited (Fig. 8a). Finally, at the scale of a stream reach or catchment, the balance
20 between light- vs. substrate-limitation of DOM degradation varies with changes in water
21 residence times, the incident UV light, and photo-lability of DOM. Our analyses indicate that
22 the hydrological and photochemical conditions in Innavait Creek create light-limitation for
23 DOM photo-degradation, and we suggest that photo-degradation in most streams and ponds with
24 high CDOM is similarly light-limited.

25 **Author contributions**

26 GWK, BTN and RMC designed the field sampling plan and all authors contributed to the field
27 work and data analysis. RMC, GWK and BTN prepared the manuscript with contributions
28 KHH.

29 **Acknowledgements**

1 Funding was provided in part by grants NFS ARC-1204220 (to BTN), NSF DEB-1026843 (to
2 GWK), NSF OPP-1022876/1023270 (to RMC and GWK), and NSF - CAREER 1255060 (to
3 RMC). We thank Jason Dobkowski, Brittany Papworth, Sara Fortin, and EDC staff at Toolik
4 Field Station for help in the field.

5 **References**

- 6 Amado, A. M., Farjalla, V. F., Esteves, F. D. A., Bozelli, R. L., Roland, F. and Enrich-Prast, A.:
7 Complementary pathways of dissolved organic carbon removal pathways in clear-water
8 Amazonian ecosystems: Photochemical degradation and bacterial uptake, *FEMS Microbiol.*
9 *Ecol.*, 56(1), 8–17, doi:10.1111/j.1574-6941.2006.00028.x, 2006.
- 10 Battin, T. J., Kaplan, L. a., Findlay, S., Hopkinson, C. S., Marti, E., Packman, A. I., Newbold, J.
11 D. and Sabater, F.: Biophysical controls on organic carbon fluxes in fluvial networks, *Nat.*
12 *Geosci.*, 2(8), 595–595, doi:10.1038/ngeo602, 2009.
- 13 Boano, F. and Harvey, J.: Hyporheic flow and transport processes: Mechanisms, models, and
14 biogeochemical implications, *Rev. Geophys.*, 603–679, doi:10.1002/2012RG000417.Received,
15 2014.
- 16 Brooks, M. L., Meyer, J. S. and McKnight, D. M.: Photooxidation of wetland and riverine
17 dissolved organic matter: Altered copper complexation and organic composition, *Hydrobiologia*,
18 579(1), 95–113, doi:10.1007/s10750-006-0387-6, 2007.
- 19 Caplanne, S. and Laurion, I.: Effect of chromophoric dissolved organic matter on epilimnetic
20 stratification in lakes, *Aquat. Sci.*, 70(2), 123–133, doi:10.1007/s00027-007-7006-0, 2008.
- 21 Chapra, S. C. and Runkel, R. L.: Modeling Impact of Storage Zones on Stream Dissolved
22 Oxygen, *J. Environ. Eng.*, 125(5), 415–419, doi:10.1061/(ASCE)0733-9372(1999)125:5(415),
23 1999.
- 24 Cole, J. J., Caraco, N. F., Kling, G. W. and Kratz, T. K.: Carbon dioxide supersaturation in the
25 surface waters of lakes., *Science*, 265(5178), 1568–1570, doi:10.1126/science.265.5178.1568,
26 1994.
- 27 Cole, J. J., Prairie, Y. T., Caraco, N. F., McDowell, W. H., Tranvik, L. J., Striegl, R. G., Duarte,
28 C. M., Kortelainen, P., Downing, J. A., Middelburg, J. J. and Melack, J.: Plumbing the global

1 carbon cycle: Integrating inland waters into the terrestrial carbon budget, *Ecosystems*, 10(1),
2 171–184, doi:10.1007/s10021-006-9013-8, 2007.

3 Cory, R. M. and Kaplan, L. A.: Biological lability of streamwater fluorescent dissolved organic
4 matter, *Limnol. Oceanogr.*, 57(5), 1347–1360, doi:10.4319/lo.2012.57.5.1347, 2012.

5 Cory, R. M., McKnight, D. M., Chin, Y. P., Miller, P. and Jaros, C. L.: Chemical characteristics
6 of fulvic acids from Arctic surface waters: Microbial contributions and photochemical
7 transformations, *J. Geophys. Res. Biogeosciences*, 112(4), doi:10.1029/2006JG000343, 2007.

8 Cory, R. M., Miller, M. P., McKnight, D. M., Guerard, J. J. and Miller, P. L.: Effect of
9 instrument-specific response on the analysis of fulvic acid fluorescence spectra, *Limnol.*
10 *Oceanogr. Methods*, 8, 67–78, doi:10.4319/lom.2010.8.0067, 2010.

11 Cory, R. M., Crump, B. C., Dobkowski, J. a and Kling, G. W.: Surface exposure to sunlight
12 stimulates CO₂ release from permafrost soil carbon in the Arctic., *Proc. Natl. Acad. Sci. U. S.*
13 *A.*, 110(9), 3429–34, doi:10.1073/pnas.1214104110, 2013.

14 Cory, R. M., Ward, C. P., Crump, B. C. and Kling, G. W.: Sunlight controls water column
15 processing of carbon in arctic fresh waters, *Science* (80-.), 345(6199), 925–928,
16 doi:10.1126/science.1253119, 2014.

17 Detterman, R. L., Bowsher, A. L. and Dutro Jr., J. T.: Glaciation on the Arctic Slope of the
18 Brooks Range, Northern Alaska, *Arctic*, 11(1), 43–61, 1958.

19 Fee, E. J., Hecky, R. E., Kasian, S. E. M. and Cruikshank, D. R.: Effects of lake size, water
20 clarity, and climatic variability on mixing depths in Canadian Shield lakes, *Limnol. Oceanogr.*,
21 41(5), 912–920, doi:10.4319/lo.1996.41.5.0912, 1996.

22 Gareis, J. a L., Lesack, L. F. W. and Bothwell, M. L.: Attenuation of in situ UV radiation in
23 Mackenzie Delta lakes with varying dissolved organic matter compositions, *Water Resour. Res.*,
24 46(9), 1–14, doi:10.1029/2009WR008747, 2010.

25 Graneli, W., Lindell, M. and Tranvik, L. J.: Photo-oxidative production of dissolved inorganic
26 carbon in lakes of different humic content, *Limnol. Oceanogr.*, 41(4), 698–706,
27 doi:10.4319/lo.1996.41.4.0698, 1996.

1 Hamilton, T. D.: Late Cenozoic glaciation of the central Brooks Range, in *Glaciation in Alaska-*
2 *The geologic record*, edited by T. D. Hamilton, K. M. Reed, and R. M. Thorson, pp. 9–50,
3 Alaska Geological Society., 1986.

4 Helms, J. R., Stubbins, A., Ritchie, J. D., Minor, E. C., Kieber, D. J. and Mopper, K.: Absorption
5 spectral slopes and slope ratios as indicators of molecular weight, source, and photobleaching of
6 chromophoric dissolved organic matter, *Limnol. Oceanogr.*, 53(3), 955–969,
7 doi:10.4319/lo.2008.53.3.0955, 2008.

8 Hinzman, L. D., Kane, D. L., Gieck, R. E. and Everett, K. R.: Hydrologic and thermal properties
9 of the active layer in the Alaskan Arctic, *Cold Reg. Sci. Technol.*, 19, 95–110, 1991.

10 Hobbie, J. E.: *Limnology of Tundra Ponds, Barrows, Alaska, US/IBP Synth. Ser. n.13* Dowden,
11 Hutchinson Ross, Inc. Stroudsbeng, PA 514 pp., 0(0), NULL, 1980.

12 Houser, J. N.: Water color affects the stratification, surface temperature, heat content, and mean
13 epilimnetic irradiance of small lakes, *Can. J. Fish. Aquat. Sci.*, 63(11), 2447–2455,
14 doi:10.1139/f06-131, 2006.

15 Hu, C. M., Muller-Karger, F. E. and Zepp, R. G.: Absorbance, absorption coefficient, and
16 apparent quantum yield: A comment on common ambiguity in the use of these optical concepts,
17 *Limnol. Oceanogr.*, 47(4), 1261–1267, 2002.

18 Judd, K., Crump, B. and Kling, G.: Bacterial responses in activity and community composition
19 to photo-oxidation of dissolved organic matter from soil and surface waters, *Aquat. Sci. - Res.*
20 *Across Boundaries*, 69, 96–107, doi:10.1007/s00027-006-0908-4, 2007.

21 Kane, D. L.: No Title, [online] Available from:
22 <http://ine.uaf.edu/werc/projects/NorthSlope/northslope.html>, 2015.

23 Kane, D. L. and Hinzman, L. D.: Climate data from the North Slope Hydrology Research
24 project, , accessed Feb. 2013 [online] Available from:
25 <http://ine.uaf.edu/werc/projects/NorthSlope>, 2011.

26 Kane, D. L., Hinzman, L. D., McNamara, J. P., Zhang, Z. and Benson, C. S.: An overview of a
27 nested watershed study in Arctic Alaska, *Nord. Hydrol.*, 31(4-5), 245–266 [online] Available
28 from: <Go to ISI>://WOS:000167153700002, 2000.

1 Kane, D. L., Gieck, R. E., Kitover, D. C., Hinzman, L. D., McNamara, J. P. and Yang, D.:
2 Hydrological cycle on the North Slope of Alaska, in Northern Research Basins Water Balance,
3 edited by D. L. Kane and D. Yang, pp. 224–236, IAHS Press, Wallingford., 2004.

4 Kling, G. W.: Comparative transparency, depth of mixing, and stability of stratification in lakes
5 of Cameroon, West Africa, *Limnol. Oceanogr.*, 33(1), 27–40, doi:10.4319/lo.1988.33.1.0027,
6 1988.

7 Kling, G. W., Kipphut, G. W. and Miller, M. C.: Arctic lakes and streams as gas conduits to the
8 atmosphere: implications for tundra carbon budgets., *Science*, 251(4991), 298–301,
9 doi:10.1126/science.251.4991.298, 1991.

10 Koehler, B., Landelius, T., Weyhenmeyer, G. a., Machida, N. and Tranvik, L. J.: Sunlight-
11 induced carbon dioxide emissions from inland waters, *Global Biogeochem. Cycles*, 28(7), 696–
12 711, doi:10.1002/2014GB004850, 2014.

13 McKnight, D. M., Boyer, E. W., Westerhoff, P. K., Doran, P. T., Kulbe, T. and Andersen, D. T.:
14 Spectrofluorometric characterization of dissolved organic matter for indication of precursor
15 organic material and aromaticity, *Limnol. Oceanogr.*, 46(1), 38–48,
16 doi:10.4319/lo.2001.46.1.0038, 2001.

17 McNamara, J. P., Kane, D. L. and Hinzman, L. D.: An analysis of streamflow hydrology in the
18 Kuparuk River Basin, Arctic Alaska: a nested watershed approach, *J. Hydrol.*, 206(1-2), 39–57,
19 doi:10.1016/S0022-1694(98)00083-3, 1998.

20 McNamara, J. P., Kane, D. L., Hobbie, J. E. and Kling, G. W.: Hydrologic and biogeochemical
21 controls on the spatial and temporal patterns of nitrogen and phosphorus in the Kuparuk River,
22 arctic Alaska, *Hydrol. Process.*, 22, 3294–3309, doi:10.1002/hyp.6902, 2008.

23 Merck, M. F. and Neilson, B. T.: Modelling in-pool temperature variability in a beaded arctic
24 stream, *Hydrol. Process.*, 26(25), 3921–3933, doi:10.1002/hyp.8419, 2012.

25 Merck, M. F., Neilson, B. T., Cory, R. M. and Kling, G. W.: Variability of in-stream and riparian
26 storage in a beaded arctic stream, *Hydrol. Process.*, 26(19), 2938–2950, doi:10.1002/hyp.8323,
27 2012.

1 Miller, M. P., McKnight, D. M., Chapra, S. C. and Williams, M. W.: A model of degradation and
2 production of three pools of dissolved organic matter in an alpine lake, *Limnol. Oceanogr.*,
3 54(6), 2213–2227, doi:10.4319/lo.2009.54.6.2213, 2009.

4 Miller, W. L.: Effects of UV-radiation on aquatic humus: photochemical principles and
5 experimental considerations, in *Aquatic Humic Substances - Ecology and Biogeochemistry*,
6 edited by D. O. Hessen and L. J. . Tranvik, pp. pp. 126–143, Springer Berlin Heidelberg., 1998.

7 Moran, M. A., Sheldon, W. M. and Zepp, R. G.: Carbon loss and optical property changes during
8 long-term photochemical and biological degradation of estuarine dissolved organic matter,
9 *Limnol. Oceanogr.*, 45(6), 1254–1264, doi:10.4319/lo.2000.45.6.1254, 2000.

10 Morris, D. P., Zagarese, H., Williamson, C., BALSEIRO, E. G., HARGREAVES, B. R.,
11 MODENUTTI, B., MOELLER, R. and QUEIMALINOS, C.: The attenuation of solar UV
12 radiation in lakes and the role of dissolved organic carbon, *Limnol. Oceanogr.*, 40(8), 1381–
13 1391, doi:10.4319/lo.1995.40.8.1381, 1995.

14 Neilson, B. T., Hatch, C. E., Ban, H. and Tyler, S. W.: Solar radiative heating of fiber-optic
15 cables used to monitor temperatures in water, *Water Resour. Res.*, 46(8), W08540,
16 doi:10.1029/2009WR008354, 2010.

17 Osterkamp, T. E. and Payne, M. W.: Estimates of permafrost thickness from well logs in
18 northern Alaska, *Cold Reg. Sci. Technol.*, 5(1), 13–27, doi:10.1016/0165-232X(81)90037-9,
19 1981.

20 Page, S. E., Kling, G. W., Sander, M., Harrold, K. H., Logan, J. R., McNeill, K. and Cory, R. M.:
21 Dark formation of hydroxyl radical in arctic soil and surface waters, *Environ. Sci. Technol.*,
22 47(22), 12860–12867, doi:10.1021/es4033265, 2013.

23 Page, S. E., Logan, J. R., Cory, R. M. and McNeill, K.: Evidence for dissolved organic matter as
24 the primary source and sink of photochemically produced hydroxyl radical in arctic surface
25 waters., *Environ. Sci. Process. Impacts*, 16(4), 807–22, doi:10.1039/c3em00596h, 2014.

26 Prairie, Y., Breton, J., Vallières, C. and Laurion, I.: Limnological properties of permafrost thaw
27 ponds in northeastern Canada, *Can. J. Fish. Aquat. Sci.*, 66(10), 1635–1648, doi:10.1139/F09-
28 108, 2009.

1 Spencer, R. G. M., Hernes, P. J., Ruf, R., Baker, A., Dyda, R. Y., Stubbins, A. and Six, J.:
2 Temporal controls on dissolved organic matter and lignin biogeochemistry in a pristine tropical
3 river, Democratic Republic of Congo, *J. Geophys. Res. Biogeosciences*, 115(3),
4 doi:10.1029/2009JG001180, 2010.

5 Stedmon, C. A., Markager, S. and Bro, R.: Tracing dissolved organic matter in aquatic
6 environments using a new approach to fluorescence spectroscopy, *Mar. Chem.*, 82(3-4), 239–
7 254, doi:10.1016/S0304-4203(03)00072-0, 2003.

8 Stubbins, A., Spencer, R. G. M., Chen, H., Hatcher, P. G., Mopper, K., Hernes, P. J., Mwamba,
9 V. L., Mangangu, A. M., Wabakanghanzi, J. N. and Six, J.: Illuminated darkness: Molecular
10 signatures of Congo River dissolved organic matter and its photochemical alteration as revealed
11 by ultrahigh precision mass spectrometry, *Limnol. Oceanogr.*, 55(4), 1467–1477,
12 doi:10.4319/lo.2010.55.4.1467, 2010.

13 Tranvik, L. J. and Bertilsson, S.: Contrasting effects of solar UV radiation on dissolved organic
14 sources for bacterial growth, *Ecol. Lett.*, 4(5), 458–463, doi:10.1046/j.1461-0248.2001.00245.x,
15 2001.

16 Vähätalo, A. V. and Wetzel, R. G.: Long-term photochemical and microbial decomposition of
17 wetland-derived dissolved organic matter with alteration of ¹³C:¹²C mass ratio, *Limnol.*
18 *Oceanogr.*, 53(4), 1387–1392, doi:10.4319/lo.2008.53.4.1387, 2008.

19 Walker, D. A., Binnian, E., Evans, B. M., Lederer, N. D., Nordstrand, E. and Webber, P. J.:
20 Terrain, vegetation and landscape evolution of the R4D research site, Brooks-Range-foothills,
21 Alaska, *Holarct. Ecol.*, 12(3), 238–261, 1989.

22 Watanabe, S., Laurion, I., Chokmani, K., Pienitz, R. and Vincent, W. F.: Optical diversity of
23 thaw ponds in discontinuous permafrost: A model system for water color analysis, *J. Geophys.*
24 *Res. Biogeosciences*, 116(2), doi:10.1029/2010JG001380, 2011.

25 Weishaar, J. L., Aiken, G. R., Bergamaschi, B. A., Fram, M. S., Fujii, R. and Mopper, K.:
26 Evaluation of specific ultraviolet absorbance as an indicator of the chemical composition and
27 reactivity of dissolved organic carbon, *Environ. Sci. Technol.*, 37(20), 4702–4708,
28 doi:10.1021/es030360x, 2003.

29 Wetzel, R. G.: *Limnology: Lake and River Ecosystems.*, 2001.

1 Zarnetske, J. P., Haggerty, R., Wondzell, S. M. and Baker, M. A.: Dynamics of nitrate
2 production and removal as a function of residence time in the hyporheic zone, *J. Geophys. Res.*
3 *Biogeosciences*, 116(1), doi:10.1029/2010JG001356, 2011.

4

5

6

7

8

Table 1. Meteorological conditions at Toolik Field Station during study periods

Period	^a Global Solar Radiation	^a UV+Visible Photon Flux	^b Air Temperature (1 m)	^a Precipitation	^c Total discharge at weir
	kW m ⁻²	mol photons m ⁻²	°C	mm	m ³
2011	12	2111	9	63	41x10 ³
2012	10	1600	10	189	233x10 ³

^aSum of daily average values from 23-June through 18-August in each year (sampling periods in 2011 and 2012).

^bDaily average value from 23-June through 18-August. ^c Sum discharge passing the weir at Imnavait from 28-Jun to 18-August.

Table 2. Annual average hydrologic and chemical characteristics of soil and stream water samples from Innavait Creek.

		Soil Water		Pool Bottom Water		Pool Surface Water	
		2011	2012	2011	2012	2011	2012
Water Temp	°C			11 ± <1	11 ± <1	14 ± 1 ^A	11 ± 1 ^B
pH		5.2 ± 0.4	5.2 ± 0.1	5.5 ± 0.1	5.6 ± 0.1	5.7 ± 0.1	5.7 ± 0.1
Conductivity	µs cm ⁻¹	26 ± 1	25 ± 2	42 ± 10 ^A	17 ± 3 ^B	13 ± <1	12 ± <1
DOC	µM C	1357 ± 110	1412 ± 78	1252 ± 85 ^A	1100 ± 17 ^B	785 ± 13 ^A	1028 ± 21 ^B
a₃₀₅	m ⁻¹	96 ± 10	87 ± 7	118 ± 19 ^A	61 ± 2 ^B	53 ± 2	53 ± 1
S_R		0.75 ± 0.01	0.74 ± 0.01	0.70 ± 0.02 ^A	0.75 ± 0.01 ^B	0.78 ± 0.02	0.76 ± <0.01
SUVA₂₅₄	(L mg C ⁻¹ m ⁻¹)	4.4 ± 0.1 ^A	4.1 ± 0.1 ^B	5.2 ± 0.5 ^A	3.9 ± 0.1 ^B	4.5 ± 0.1 ^A	3.7 ± <0.1 ^B
Peak A	RU	3.3 ± 0.2	2.9 ± 0.2	3.5 ± 0.1 ^A	2.8 ± <0.1 ^B	2.5 ± <0.1 ^A	2.7 ± 0.1 ^B
FI		1.59 ± 0.01	1.60 ± 0.01	1.55 ± 0.01 ^A	1.57 ± 0.01 ^B	1.51 ± 0.01 ^A	1.55 ± <0.01 ^B

All values are seasonal averages ± standard error across all dates in 2011 or 2012. Letters indicate significant difference ($p < 0.05$) in mean values between years (2011 vs. 2012) for each water type (soil waters, pool bottom waters, and pool surface waters).

Table 3. DOM in soil waters compared to pool water in Innavait Creek under stratified conditions

		Soil Water	Pool Bottom Water	Pool Surface Water
DOC	$\mu\text{M C}$	1382 ± 69	1188 ± 56	815 ± 12
a_{305}	m^{-1}	92 ± 6	100 ± 13	50 ± 1
S_R		0.75 ± 0.01	0.71 ± 0.01	0.77 ± 0.01
SUVA₂₅₄	$(\text{L mg C}^{-1} \text{ m}^{-1})$	4.4 ± 0.1	4.9 ± 0.3	4.2 ± 0.1
Peak A	RU	3.1 ± 0.2	3.2 ± 0.1	2.38 ± 0.05
FI		1.60 ± 0.01	1.57 ± 0.01	1.52 ± 0.01

All values shown as average \pm standard error; calculated in the pool surface or bottom across all dates in 2011 and 2012 when pools were stratified (2011: 27-Jun, 29-Jun, 14-Jul, 4-Aug; 2012: 23-Jun, 30-Jun). Soil water means were calculated from over both years (2011-2012). All water types were statistically different from one another for all variables (ANOVA $p < 0.01$).

Table 4. Effect of sunlight and bacteria on CDOM, FDOM and DOM mineralization.

Process	a_{305} m^{-1}	S_R	$SUVA_{254}$ $L\ mg\ C^{-1}\ m^{-1}$	FI	Peak A RU	Peak C RU	Peak T RU	Mineralization rate ($mmol\ C\ m^{-2}\ d^{-1}$)
^a Photo-degradation	-12.4 ± 1.8	15.8 ± 1.3	-4.9 ± 0.01	-11.7 ± 0.8	-12.1 ± 1.4	-27.2 ± 2.1	4.1 ± 1.5	24.7 ± 18.3
^b Bacterial degradation	-2.9 ± 1.6	ND	5.0 ± 0.03	ND	-7.6 ± 2.4	-3.6 ± 1.5	-2.5 ± 8.2	2.35 ± 0.34
^c Photo + bacterial degradation	3 ± 1	1 ± 1	NM	5 ± 1	7 ± 1	15 ± 1	-12 ± 1	3.04 ± 1.31

DOM degradation quantified as percent change in CDOM or FDOM of Innavait Creek waters after ^aexposure to 12 h sunlight compared to dark control (photo-degradation), ^b after seven days of incubation of whole waters at 6-7 °C compared to killed control (bacterial degradation), or ^c after 12 h sunlight followed by seven days of incubation with natural bacterial community in stream water at 6-7 °C relative to killed controls (here the percent change is relative to the initial photo-exposed water). Data shown as average \pm standard error of three photochemical experiments, two bacterial incubations, and one coupled photo-bacterial incubation. Within each of the bacterial or photo + bacterial experiments there were four replicates per treatment (light, dark, live or killed controls). ND = none detected based on no significant difference compared to killed controls. NM = not measured.

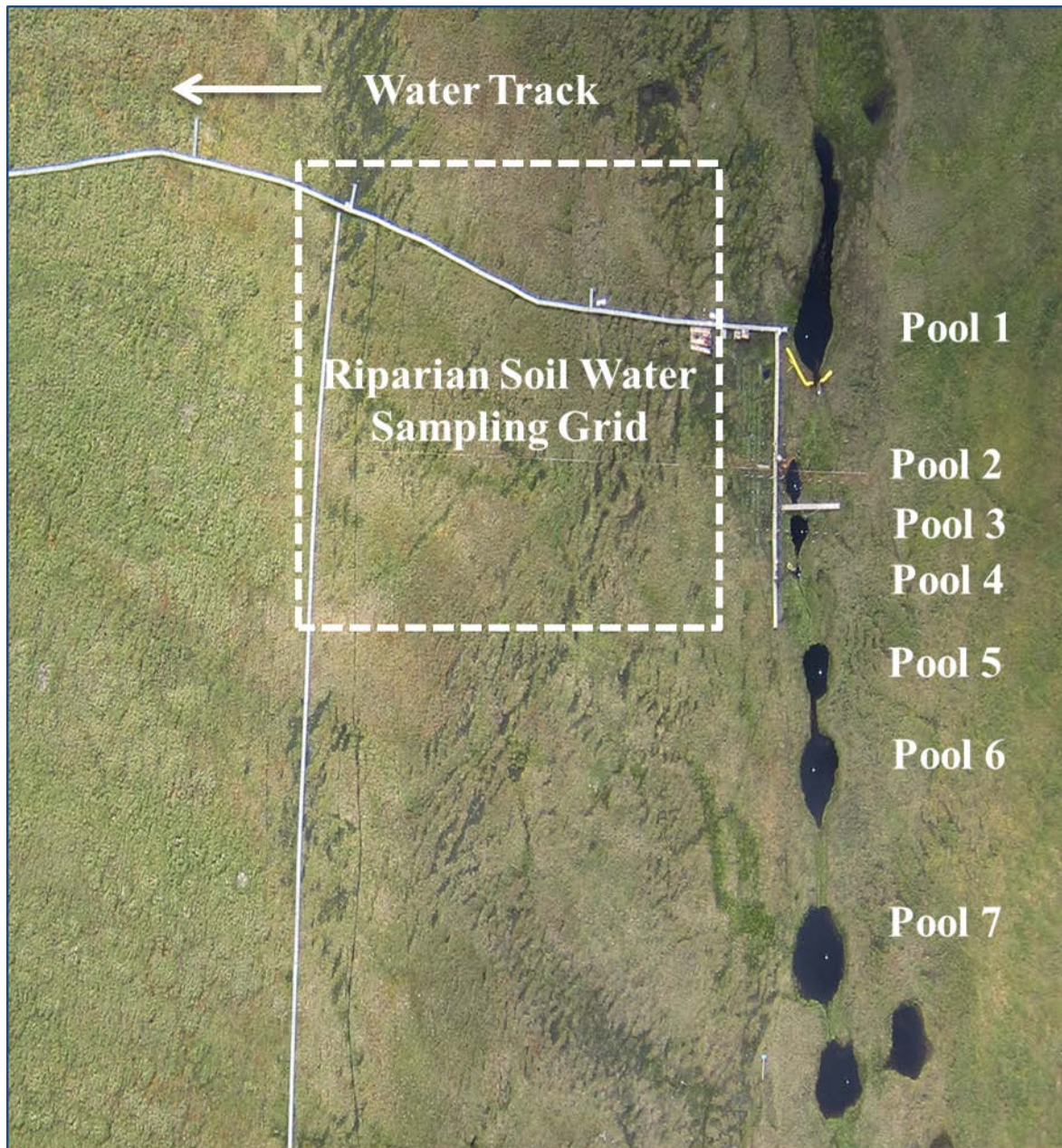


Fig. 1. Study area showing the 120 m reach of Innavait Creek containing seven consecutive pools, and the locations of soil water collection (riparian zone and water track; only the bottom portion of the water track is shown in this image). Also visible in this areal image as white solid lines are boardwalks installed to access sampling sites.

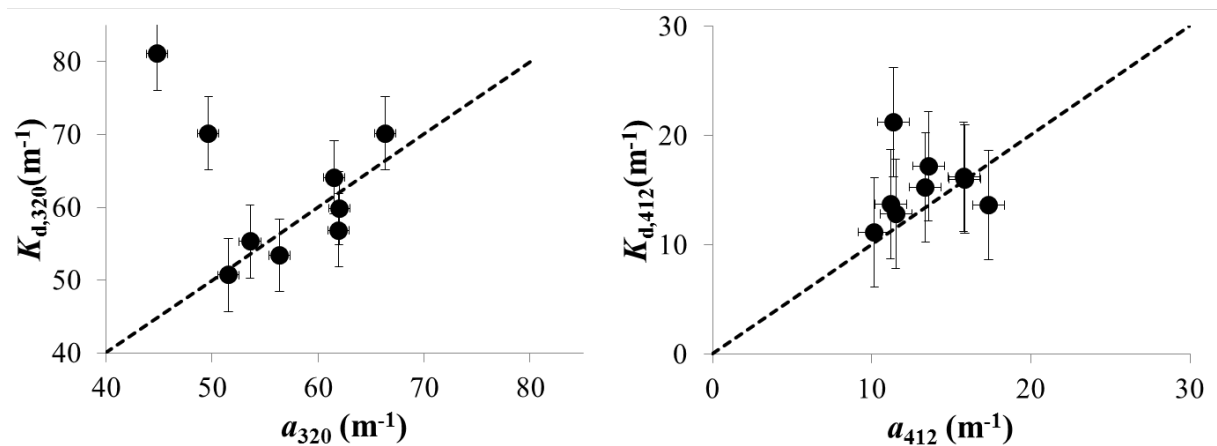


Fig. 2. $K_{d,\lambda}$ vs. $a_{\text{CDOM},\lambda}$ at 320 nm (left) and 412 nm (right) plotted vs. 1:1 line (dotted line). $a_{\text{CDOM},\lambda}$ measured on the laboratory spectrophotometer was corrected for the average cosine of downwelling radiation for the time of day (i.e., zenith angle) that the in-situ $K_{d,\lambda}$ values were measured in Innavait Creek. Thus $a_{\text{CDOM},\lambda}$ values in this figure are not directly comparable to the values presented in Tables 2 and 3.

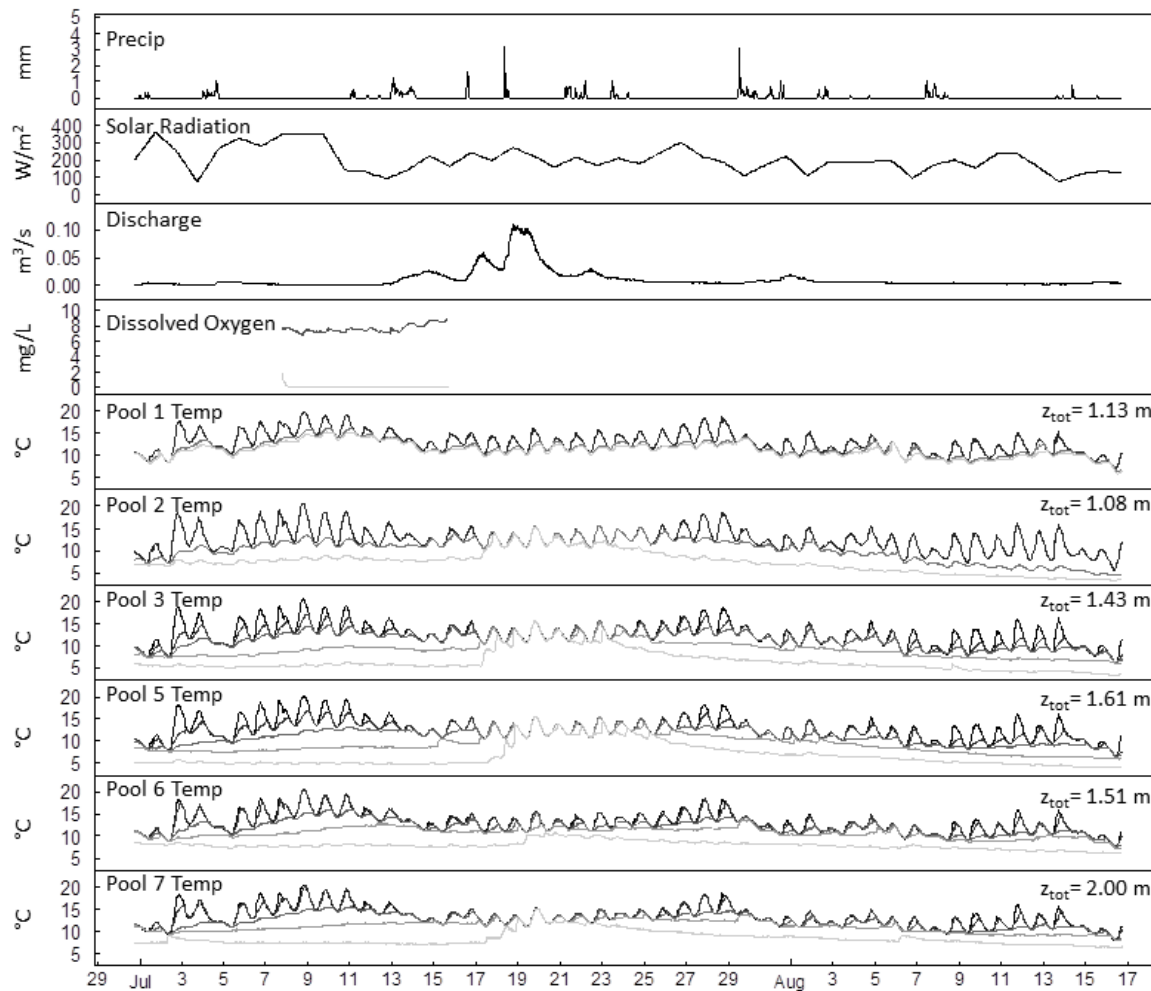


Fig. 3. Innavaik Creek precipitation, solar radiation, discharge (at location downstream of study reach), dissolved oxygen in pool 2 top and bottom, and vertical arrays (VA) of temperature sensors within each study pool (P) in summer 2011. The darkest lines represent the sensor at the top of the water column; subsequent lines become lighter with depth of each sensor. The sensors were placed in each pool starting 5 to 15 cm from the bottom of the pool and then at intervals ranging from 5 to 50 cm over the depth of each pool (z_{tot}) as indicated in the figure.

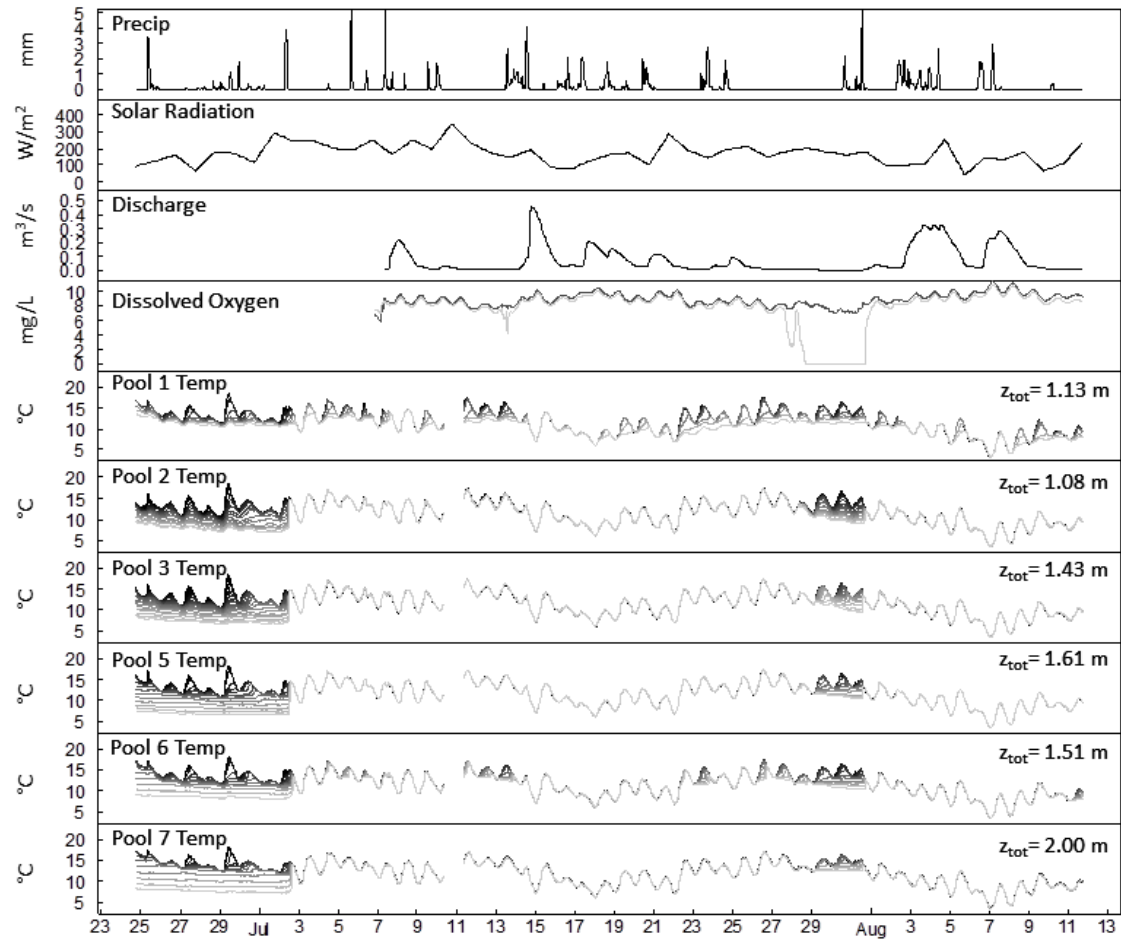


Fig. 4. Innavait Creek precipitation, solar radiation, discharge (at location downstream of study reach), dissolved oxygen in pool 2 top and bottom, and vertical arrays (VA) of temperature sensors within each study pool (P) in summer 2012. The darkest lines represent the sensor at the top of the water column; subsequent lines become lighter with depth of each sensor. The sensors were placed in each pool starting 5 to 15 cm from the bottom of the pool and then at intervals ranging from 5 to 50 cm over the depth of each pool (z_{tot}) as indicated in the figure.

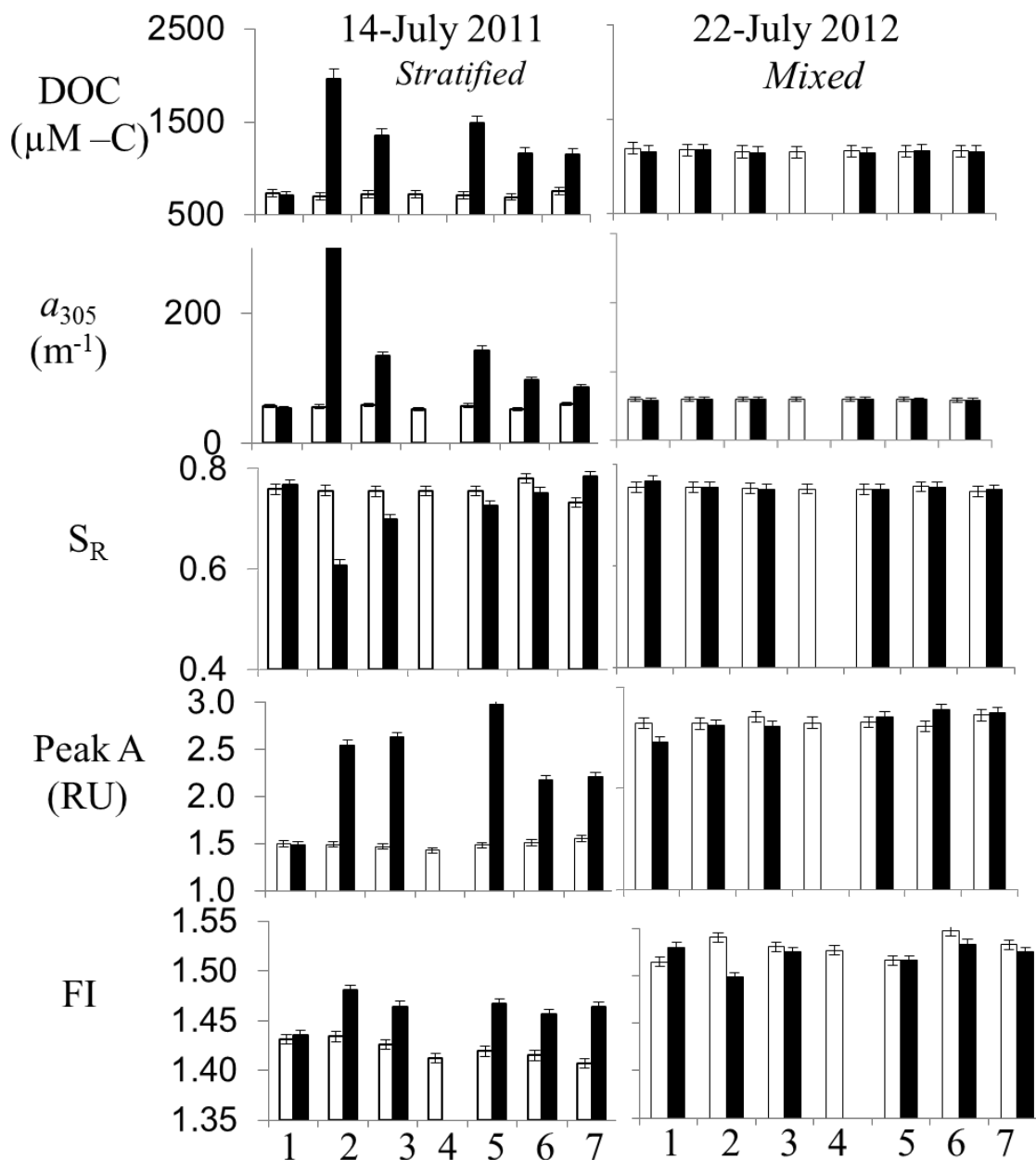


Fig. 5. Concentration and quality of DOM in the surface (open bars) and bottom waters (filled bars) in pools 1-7 in Innavait Creek under stratified (left) and mixed (right) conditions in 2011 and 2012, respectively. CDOM and FDOM concentrations shown as absorption coefficients at 305 nm (a_{305}) and emission intensities at Peak A (Raman Units; RU), respectively. DOM quality shown as slope ratio (S_R) and fluorescence index (FI); CDOM and FDOM proxies for DOM described in text.

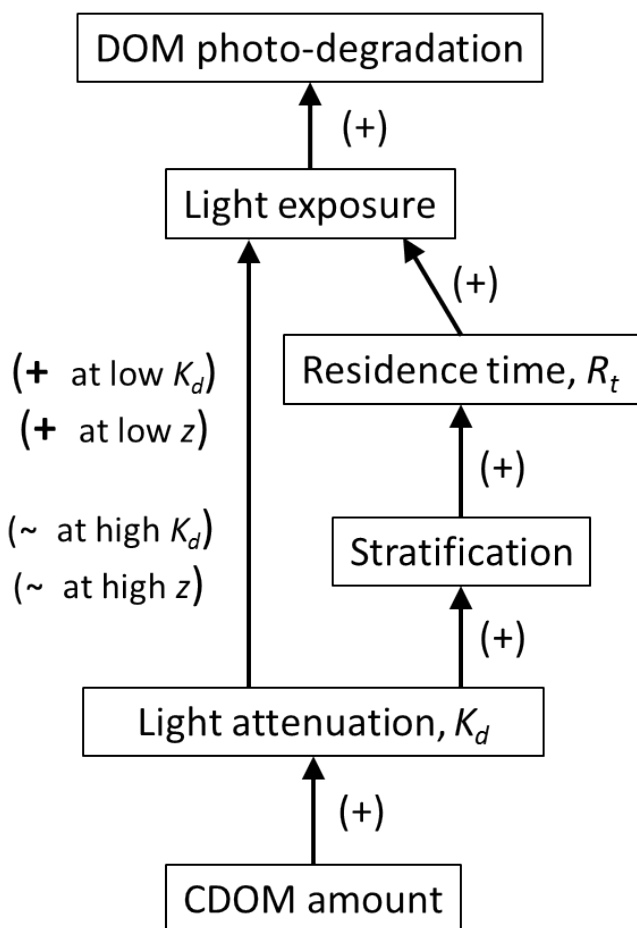


Fig. 6. Conceptual diagram illustrating the controls on DOM photo-degradation. As CDOM increases it absorbs more light at the surface and strengthens stratification, which increases residence times, length of light exposure, and thus DOC photo-degradation (right side). Similarly, as CDOM and thus light attenuation increase the total amount of light exposure and light absorption increases in situations where there is low K_d or shallow water column depth z . However, as K_d or shallow water column depth increase the system becomes light limited, and further increases in CDOM result in no change in DOM photo-degradation (asymptote of Fig. S1).

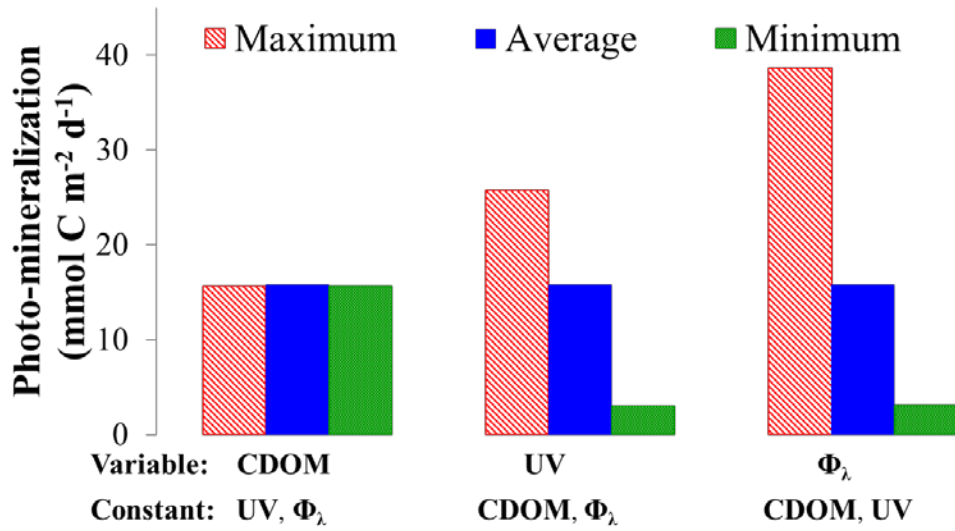


Fig. 7. Effect of CDOM, incident UV, and Φ_λ (apparent quantum yield) on water column rates of photo-mineralization of DOM to CO_2 in Innavait Creek. For each scenario, two variables from *Eqn. 3* were held constant, and one was varied using the average, minimum, and maximum values observed over the study period at Innavait Creek (2011-2012). UV = daily total UV reaching water surface at Innavait Creek (dependent on solar zenith angle and cloud cover).

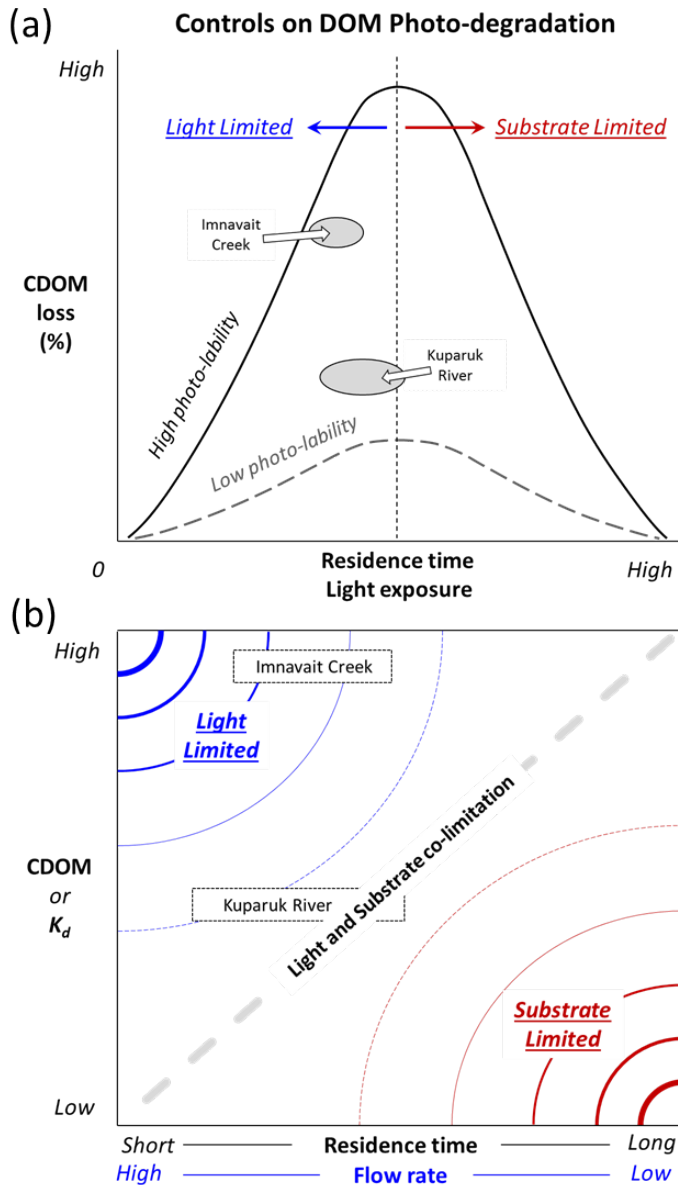


Fig. 8. Controls on DOC photo-degradation. **(a)** As residence time or light exposure increase, so does DOC photo-degradation (% loss of the initial pool of CDOM, without replacement). The CDOM loss for any given light exposure is greater for higher photo-labile DOC (solid line) than it is for lower photo-labile DOC (dashed line). At low light exposure levels photo-degradation is “light-limited”, but after sufficient CDOM is lost the process switches to be “substrate-limited” (insufficient CDOM). **(b)** This shows the light- vs. substrate- limitation in terms of CDOM concentrations or light attenuation (K_d), Y-axis, and the water residence time or flow rate (X-axis). At high CDOM and short residence time there is insufficient light available for photo-degradation (upper left), while at low CDOM concentrations and long residence times there is abundant light yet insufficient CDOM. The range of conditions for DOC photo-degradation in Imnavait Creek is likely always light-limited, while in the Kugaruk River conditions may be substrate-limited at times.

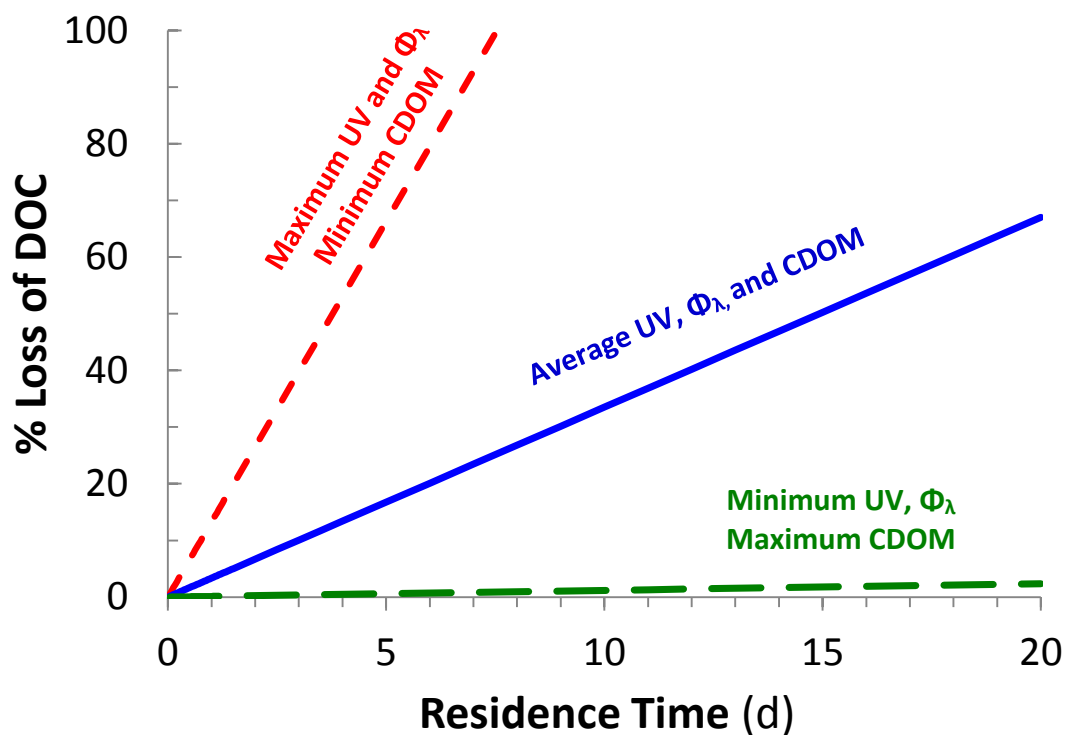


Fig. 9. Cumulative percent of DOC loss in Innavait Creek lost through photo-mineralization as calculated from *Eqn. 3* (removal of DOC as $\text{mol C m}^{-2} \text{d}^{-1}$ over the mean depth in Innavait Creek; 0.5 m) in Innavait Creek using combinations of the range of surface UV light exposure, CDOM concentrations, and apparent quantum yields (Φ_λ) measured in this study for up to a 20 day residence time. For each scenario, the initial DOC concentration was set to $943 \mu\text{M C}$, the average surface water DOC concentration over both 2011 and 2012 (Table 2). Calculations do not include (1) the effect of DOC loss on changing light attenuation (K_d) over the residence time (i.e., CDOM and thus $K_{d,\lambda}$ remain constant over the residence time for each scenario), or (2) the effect of UV light exposure on Φ_λ over time (Φ_λ , or DOM lability, remained constant over the residence time for each scenario).